Palaeogeography, Palaeoclimatology, Palaeoecology 549 (2020) 109128

Contents lists available at ScienceDirect

Palaeogeography, Palaeoclimatology, Palaeoecology

journal homepage: www.elsevier.com/locate/palaeo

Quantifying the community turnover of the uppermost Wenlock and Ludlow (Silurian) conodonts in the Baltic Basin

Andrej Spiridonov[a,b,*], Jovita Samsonė[a], Antanas Brazauskas[a], Robertas Stankevič[a], Tõnu Meidla[c], Leho Ainsaar[c], Sigitas Radzevičius[a]

[a] Department of Geology and Mineralogy, Faculty of Chemistry and Geosciences, Vilnius University, M. K. Čiurlionio 21/27, LT-03101 Vilnius, Lithuania
[b] Laboratory of Bedrock Geology, Nature Research Centre, Akademijos str. 2, LT-08412 Vilnius, Lithuania
[c] Department of Geology, University of Tartu, Ravila 14a, 50411 Tartu, Estonia

ARTICLE INFO

Keywords:
State shift
Extinction events
Macroecology
Recurrence plots
Quantitative stratigraphy
East Baltic

ABSTRACT

The Homerian to Ludfordian interval of the mid to late Silurian Period was a time of significant changes in conodont communities, global climate, oceanographic patterns and biogeochemical cycles. The Mulde and the Lau events are preeminent examples of globally recognized conodont extinction episodes from this interval in Earth's history. The Silurian Baltic Basin is the most suitable locality, globally, for studying these perturbations to the ocean-atmosphere system, since there is an extensive record of conodont taxa occurrences, their communities, and their environments spanning across shore-face to open-ocean settings. In this study, we present new conodont and $\delta^{13}C$ data from the upper Homerian to Ludlow interval from two core sections – Gėluva-99 and Gėluva-118, representing shelfal environments, and the numerical conodont data from the Viduklė-61 section, from deep-water settings, and compare them with patterns of conodont diversity change, as revealed in the data-rich Milaičiai-103 core section. For this purpose, we explored the stratigraphically tied time series of conodont diversity changes employing recurrence and cross-recurrence plots – the binary similarity matrices that are used for deciphering complex spatial and temporal dynamic patterns. The cross-recurrence plots were used as a means of synchronizing the geological sections by applying dynamic time warping and the newly described moving window median recurrence point search algorithms. The results revealed that the conodont community compositional data are sufficiently temporally and spatially coherent to be reasonably used for synchronizing geological records. Moreover, the sudden state transitions detected in the cross-recurrence plots suggest that the Lau Event was of great importance for conodont community evolution in the studied time slice.

1. Introduction

The late Homerian to Ludlow time interval has recently enjoyed considerable interest, as it has been shown in a wide range of studies (beginning in the early nineteen-eighties) that this relatively short span of the Silurian was characterized by world-wide turnovers of biota coupled with some of the strongest positive carbon isotopic excursions and other biogeochemical perturbations, as well as probable significant sea level changes, throughout the whole Paleozoic (Aldridge et al., 1993; Calner, 2008; Calner and Jeppsson, 2003; Calner et al., 2012; Cramer et al., 2006; Eriksson et al., 2009; Frýda and Manda, 2013; Jarochowska and Munnecke, 2016; Jeppsson, 1990, 1998; Jeppsson, 2005; Jeppsson and Aldridge, 2000; Jeppsson et al., 1995; Jeppsson and Calner, 2002; Jeppsson et al., 2012; Jeppsson et al., 1994; Kozłowski, 2015; Lehnert et al., 2007a; Lehnert et al., 2007b; Loydell, 1998; Loydell et al., 2001; Martma et al., 2005; Radzevičius et al., 2016; Radzevičius et al., 2014b; Ruban, 2017; Samtleben et al., 2000; Spiridonov, 2017; Spiridonov et al., 2017a; Sullivan et al., 2016; Štorch et al., 2014; Talent et al., 1993; Zenkner and Kozłowski, 2017). These significant Earth system changes that took place during the late Wenlock to Ludlow constitute a larger pattern of general high-magnitude, possibly quasiperiodic, perturbations in the global carbon cycle, climate, oceanography and macroevolutionary rates which characterize the whole Silurian period (Cooper et al., 2014; Crampton et al., 2016; Crampton et al., 2018; Emsbo, 2017; Jeppsson, 1997; Lehnert et al., 2010; Lenton et al., 2016; Makhnach et al., 2018; Racki et al., 2012; Spiridonov et al., 2015; Spiridonov et al., 2016; Trotter et al., 2016; Vandenbroucke et al., 2015; Žigaitė et al., 2010) and possibly most of

* Corresponding author at: Department of Geology and Mineralogy, Faculty of Chemistry and Geosciences, Vilnius University, M. K. Čiurlionio 21/27, LT-03101 Vilnius, Lithuania.
E-mail address: andrej.spiridonov@gf.vu.lt (A. Spiridonov).

https://doi.org/10.1016/j.palaeo.2019.03.029
Received 28 February 2018; Received in revised form 18 March 2019; Accepted 18 March 2019
Available online 20 March 2019
0031-0182/

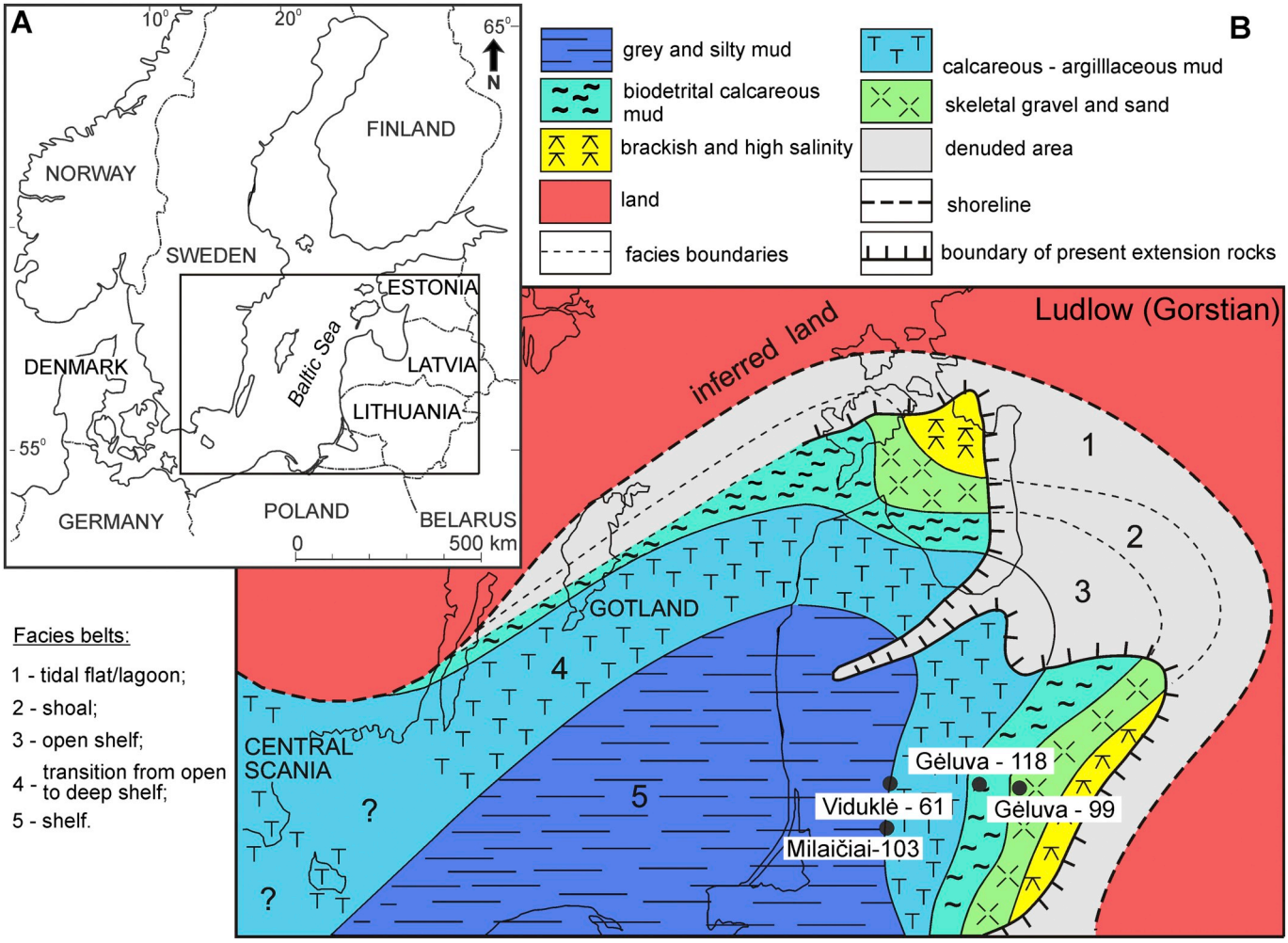

Fig. 1. Paleogeographical map (Bassett et al., 1989) showing the distribution of the studied cores: Viduklė-61, Milaičiai-103, Gėluva-99 and Gėluva-118.

the Paleozoic, which was characterized by much more volatile macroevolutionary dynamics than the rest of the Phanerozoic (Gilinsky, 1994; Lieberman and Melott, 2013; Newman and Eble, 1999), as well as by abundant high-magnitude $\delta^{13}C$ excursions (Bachan et al., 2017; Saltzman, 2005; Saltzman and Thomas, 2012).

Graptolites in offshore environments and conodonts in more nearshore settings are the primary biostratigraphical time markers of the Silurian period (Melchin et al., 2012; Sadler et al., 2009). Therefore, the fossil record of these clades forms the basis for recognizing Silurian extinction and turnover events (Jaeger, 1991; Jeppsson, 1998; Kaljo et al., 1996; Koren', 1987; Koren and Urbanek, 1994; Melchin et al., 1998; Urbanek, 1993; Urbanek et al., 2012). Nevertheless, other groups such as brachiopods, polychaetes, green algae, radiolarians and acritarchs reveal that the proposed Silurian events were not limited in their effect to the most biostratigraphically studied groups (Munnecke et al., 2012; Porębska et al., 2004; Spiridonov et al., 2017c; Stricanne et al., 2004; Tetard et al., 2017; Tonarova et al., 2012; Venckutė-Aleksienė et al., 2016). A similar proliferation of microbial sedimentary structures (e.g., stromatolites) in the aftermath of these events also reveals the presence of episodes of significant stress on the biosphere, similar to those experienced during major mass extinctions and their aftermaths (Baud et al., 2007; Calner, 2005; Chatalov, 2017; Jeppsson et al., 2007; Lapinskas, 2000; Schubert and Bottjer, 1992). Usually, low conodont abundance and diversity during the recovery phases of the discussed extinction episodes (Barrick et al., 2009, 2010), as well as changes in their abundance distributions, suggest reduced ecosystem complexity (Spiridonov et al., 2017a) and possible "mass rarity" states (Spiridonov, 2017) of the ocean (sensu Hull et al., 2015) during those times.

Understanding the mechanisms, timing and spatial synchronicity (Trubovitz and Stigall, 2016) of the described large-scale oceanic-climatic perturbations, which took place during the Silurian, in light of modern paleobiogeographical speciation theory (Lieberman et al., 2007; Stigall, 2015; Stigall et al., 2017; Vrba, 1993; Vrba and DeGusta, 2004) is of utmost importance. They can reveal the geobiological controls of metapopulation and metacommunity disturbance, differentiation and, thus, ultimately, the fabric of the macroevolution of species origination and extinction (Allmon, 2001; McKinney and Allmon, 1995; Schmitz et al., 2008; Wood and Erwin, 2017).

In this contribution, we present conodont diversity and abundance, and carbonate $\delta^{13}C$ data from two newly studied cores (Gėluva-99 and Gėluva-118) from the proximal part of the south-eastern Silurian Baltic Basin, as well as updated numerical abundance and diversity data for conodonts from the well-studied Viduklė-61 core, and compare them with the published results from the Milaičiai-103 core section. These new data, together with the published sources, are later used for testing the spatial coherence hypothesis of conodont biodiversity change in later part of Wenlock and Ludlow in the Silurian Baltic Basin. For this purpose, we used an integrated stratigraphical framework which utilizes classical conodont biostratigraphical data (ranges of time-specific taxa), chemostratigraphy and lithostratigraphy as a temporal framework for evaluating the synchronicity of changes in four studied localities from differing facies zones. In order to achieve this goal, we used multivariate techniques of non-metric multidimensional scaling and recurrence plots in order to decipher the conodont community

compositional dynamics. The patterns of across location similarity were explored using cross-recurrence plots, and two time series synchronization techniques, one of which is new and described in this contribution. The results of the numerical analyses were later used in evaluating the significance of the late Homerian to the latest Ludfordian biotic events on conodont evolution and the development of their communities. The revealed congruence of patterns in community change, as is shown, has important ramifications for quantitative biostratigraphical correlation using community compositional data.

2. Geological setting

Silurian sections now in Lithuania were located in the eastern part of the Baltic Basin on the western border of the Baltica palaeocontinent, which was located on the equator during the late Wenlock and Ludlow (Cocks and Torsvik, 2005). The shallow marine environments are represented in the eastern part (Fig. 1) and open marine in the western part of Lithuania (Paškevičius et al., 1994).

The new $\delta^{13}C$ isotope and conodont material comes from the Gėluva-118 (55° 15′ 48.09″ N, 22° 38′ 11.96″ E) and Gėluva-99 (55° 15′ 48.09″ N, 22° 38′ 11.96 E) wells. The most complete (since there is no evidence of major hiatuses and it spans the longest time in the studied interval) geological section is the Viduklė-61 core (55° 23′ 43.05″ N, 22° 54′ 37.01″ E), which is used as a keystone in this study. The investigated interval includes the Jaagarahu (upper part) and the Gėluva regional stages of the upper Wenlock and the Dubysa and Pagėgiai regional stages of the Ludlow in the Viduklė-61 well (Fig. 2). There, the Riga Formation with the Ančia Member can be distinguished in the upper part of the Jaagarahu Regional Stage. The Ančia Member is represented by microlaminated limestone. The Siesartis Formation represents the Gėluva Regional Stage and is composed of marl. The Dubysa Regional Stage is represented by the Dubysa Formation. The Dubysa Formation is composed of marl and limestone with different concentrations of clayey material. Overall, the amount of clayey material decreases from the lower part to the upper part of the Dubysa Formation. There, the Mituva and the Ventspils formations can be distinguished in the Pagėgiai Regional Stage. The Mituva Formation is represented by clayey limestone in the lower part and by undulated limestone in the upper part. The Ventspils Formation is composed of nodular limestone.

The Gėluva-118 well is located in central Lithuania and represents an open shelf environment (Fig. 1). According to the conodont fauna Gėluva, the Dubysa and Pagėgiai regional stages can be distinguished in the Gėluva-118 well (Fig. 3). The Gėluva Formation is composed of clayey limestone. The Dubysa Formation can be distinguished in the Dubysa Regional Stage and is composed of clayey limestone in the lower part, dolomitical marl in the middle part and clayey limestone with dolomite layers. There, the Neris Formation can be distinguished in the Pagėgiai Regional Stage. The Neris Formation is represented by dolostones with clayey limestone interbeds.

The Gėluva-99 well site is located a few kilometers to the east of the Gėluva-118 well site. The Gėluva, Dubysa and Pagėgiai regional stages are distinguished based on the conodont fauna. The Gėluva Regional Stage is represented by the Gėluva Formation, which is composed of marl and undulated and nodular limestone. There, the Dubysa Formation can be distinguished in the Dubysa Regional Stage. The Dubysa Formation is composed of undulated limestone in the Gėluva-99 core. There, the Neris Formation can be distinguished in the uppermost (few meters) part of the section. The Neris Formation is represented by undulated and nodular limestone. For a more detailed description of these formations, the reader is advised to consult Brazauskas (1987) and Paškevičius (1997).

3. Materials and methods

3.1. Conodont data

The conodont material comes from four cores. The conodont data, which consist of 126 samples from the Milaičiai-103 (55° 15′ 48.09″ N, 22° 38′ 11.96″ E) core, span the upper part of the Gorstian to the whole Ludfordian stages (between 1301 and 1155 m) and were published and thoroughly described in a previous paper (Spiridonov et al., 2017b). The Viduklė-61 core data span the uppermost Wenlock to the Ludlow series and consists of 193 samples, spanning 234.3 m and amounting to 2557 conodont elements recognized at the species level. Part of the data (upper Homerian Stage) were previously presented in an integrated stratigraphical study (Radzevičius et al., 2014a) and are also augmented by older data (Brazauskas, 1986) and some unpublished works (Brazauskas, 1993). Most of the sample weights of this core were not recorded, but they were kept within the range of 250–400 g. The data from the Gėluva-99 core consisted of 79 samples (sum total 1784 recognizable conodont elements), which spanned the uppermost Homerian and the entire Ludlow an interval of between 858.9 and 750.2 m (108.7 m). The weights of the samples from this core were also not recorded, although the sample sizes were very similar to the other core samples in this study (300–400 g). The Gėluva-118 section is represented by 77 samples with 1673 recognizable elements spanning the uppermost Homerian and the entire Ludlow an interval between 1006.6 and 847.3 m (159.3 m). The weights of these core samples were recorded, with an average sample weighing 348 g. Conodont abundance data from the Gėluva-99, Gėluva-118 and Viduklė-61 cores can be accessed in the *Supporting Information*.

All of conodont samples were prepared using the standard technique of buffered formic acid solution (Jeppsson and Anehus, 1995) and later they were washed with water. Conodont elements were handpicked from the dried residue and identified under a binocular microscope. Conodont elements of stratigraphically important taxa were photographed using a scanning electron microscope at the Nature Research Centre (Vilnius). The conodont collections studied in this contribution are being stored in the Geological Museum at Vilnius University.

3.2. $\delta^{13}C_{carb}$ data

For stable carbon and oxygen isotopic chemostratigraphy, bulk carbonate samples from the intervals of the Gėluva-99 and Gėluva-118 core sections were analyzed. The samples were taken from a micritic matrix avoiding any secondary structures (i.e., veins). For each sample, an average 2 g of rock was powdered. The samples were analyzed using a Delta V Advantage mass spectrometer with GasBench II by Thermo Scientific for preparing gases. The international standards used for the raw data calibration are: NBS 18 ($\delta^{13}C = -5.014‰$; $\delta^{18}O = -23.2‰$), NBS 19 ($\delta^{13}C = +1.95‰$; $\delta^{18}O = -2.20‰$) and LSVEC ($\delta^{13}C = -46.6‰$; $\delta^{18}O = -26.7‰$). The accuracy of the analyses is in the order of $\sigma = 0.02‰$.

The mass spectrometry analyses were conducted at the Department of Geology at the Institute of Ecology and Earth Sciences at the University of Tartu. Only stable carbon isotopic data were used in this project. The $\delta^{13}C$ and $\delta^{18}O$ data from the Gėluva-99, and Gėluva-118 cores can be found in the *Supporting Information*.

3.3. Numerical techniques of paleoecological analysis and stratigraphy

3.3.1. General remarks on data processing

In the quantitative diversity analyses, we formally equated forms with the prefix aff. as belonging to the same species lineage as those without it. On the other hand, all distinct subspecies were treated as separate evolutionary entities – species lineages (Allmon and Yacobucci, 2016; Miller III, 2016), since they represent discrete and

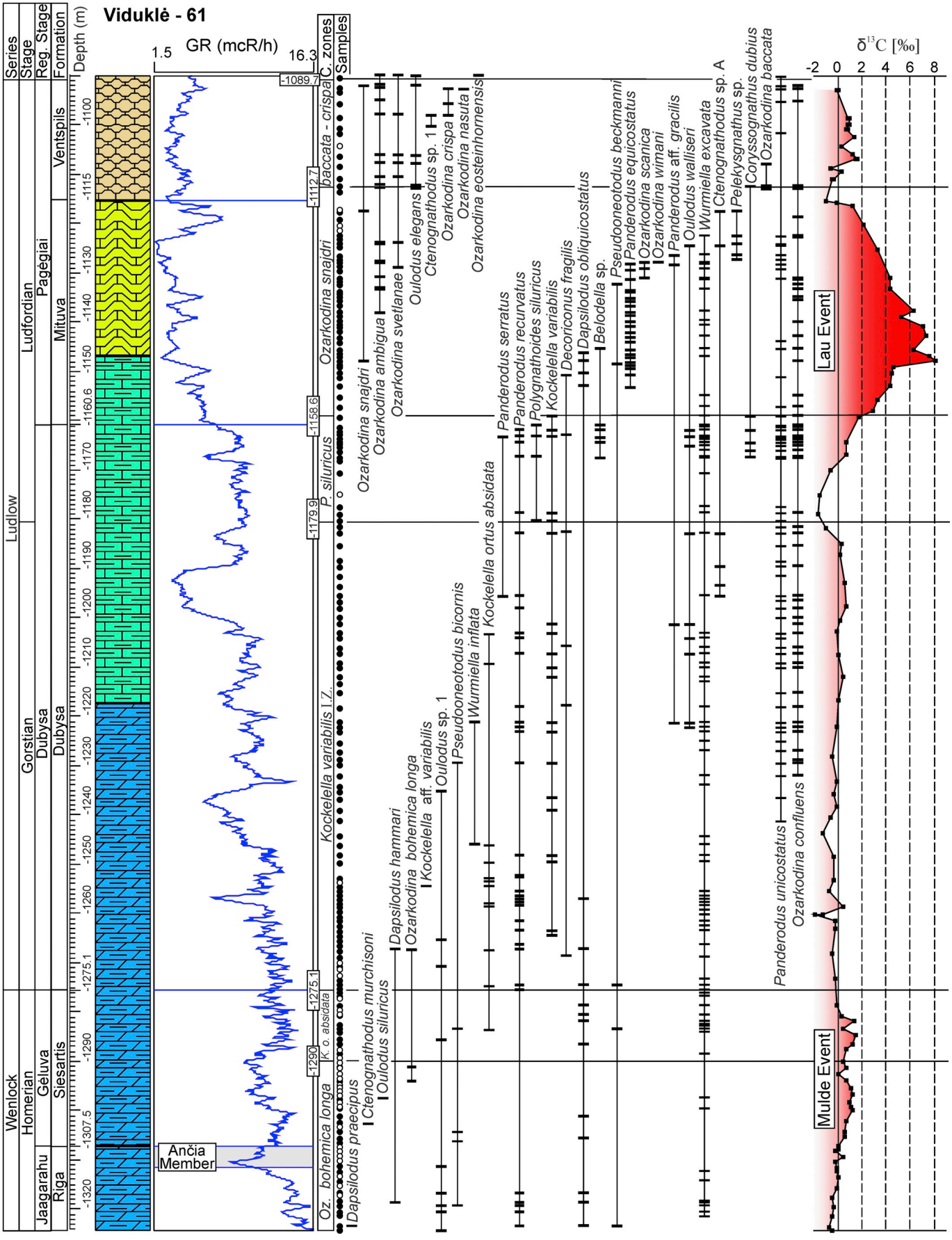

(caption on next page)

Fig. 2. Stratigraphical scheme for the upper Homerian and Ludlow of the Viduklė-61 core. From left to right: chronostratigraphic and lithostratigraphic subdivisions; lithology; gamma ray curve; conodont distributions (partially based on Radzevičius et al., 2014a); and the $\delta^{13}C$ curve (Martma et al., 2005). See the lithology legend in Fig. 4.

readily recognizable phenotypes which were probably separate species during their lifetimes (bearing in mind that they often overlap in their temporal ranges in the same sections, which is a contradiction of the definition of a subspecies).

The numerical species abundance data – the numbers of elements of any given species per sample – were used for the multivariate compositional analyses. It was shown in previous taphonomic studies that, although temporal and spatial averaging at the sample level make abundance time series more autocorrelated (Olszewski, 2012; Tomašových and Kidwell, 2010), as a rule they do not significantly disturb original species abundance profiles (Kidwell, 2001) and probably are more representative of long-term ecological states than modern "snapshot" samples from neontological studies (Holland, 2017). This is also true for the conodont material, where even local gradients in community differences are usually preserved (Vierek and Racki, 2011). Possibly low levels of Paleozoic temporal averaging (Kowalewski and Bambach, 2008), which are related to the lower abundance (than in the post-Paleozoic) of highly energetic burrowers (Allmon and Martin, 2014; Bambach, 1993), also enable the preservation of the original paleobiological and paleoclimatic signals in the fossil record.

3.3.2. Recurrence and cross-recurrence plots approaches and quantitative biostratigraphical techniques

Quantitative stratigraphy has developed an impressive array of tools over the last few decades for solving often convoluted stratal patterns of faunal (and any other) similarity, and yields compromise models for strata successions. Computational cyclostratigraphy and astrochronology are powerful tools which utilize paleoclimatic (mostly the Milankovitch spectral band) signals for manually augmented, or automatically correlated, relatively uniformly stratified geological sections (Hinnov and Hilgen, 2012; Kodama and Hinnov, 2014; Meyers et al., 2008). This approach has enjoyed some success in correlating the graptolite facies succession of part of the currently studied interval in western Lithuania (Radzevičius et al., 2017). This mode of stratigraphical inference is of great importance in situations where there are relatively small distortions in stratigraphic continuity and there are relatively minor variations in sedimentation rates on the studied timescales (tens of thousands to millions of years). Therefore, these techniques should be treated with caution when applying them to shore-face environments.

Those quantitative biostratigraphical approaches that use first and last appearance events of species could achieve very high precision and accuracy in constructing quantitative time scales (Agterberg and Gradstein, 1999; Alroy, 2000; Puolamäki et al., 2006; Sadler, 2004; Shaw, 1964), and especially when combining models with other types of data (Sadler, 2012). In this case, the exact matching of sequences is strongly dependant on the number of observed originations and extinctions at any given interval or place, and on the existence of short-lived (in relation to the desired resolution) taxa. Restricted environments and post-extinction intervals could be problematic for this kind

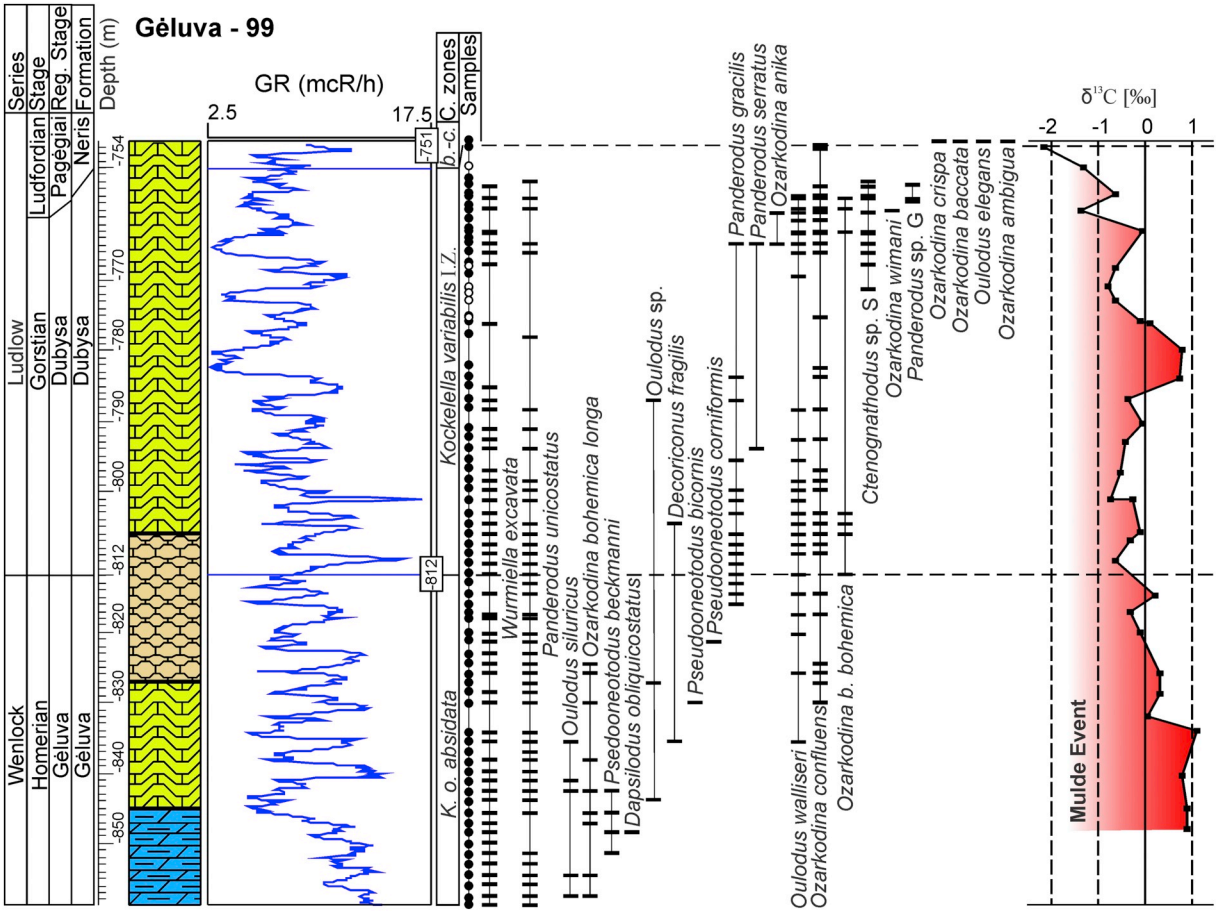

Fig. 3. Stratigraphical scheme for the upper Homerian and Ludlow of the Gėluva-99 core. From left to right: chronostratigraphic and lithostratigraphic subdivisions; lithology; gamma ray curve; conodont distribution; and $\delta^{13}C_{carb}$ curve. See the lithology legend in Fig. 4.

of stratigraphical analysis (Girard and Renaud, 2007). However, other approaches which use community compositional data by utilizing the combinatorial matching of samples through their similarities could be used effectively in the fine-scale correlation of communities (Sheets et al., 2012). With this approach, environmental faunal gradients and paleobiogeographical patterns would probably be significant obstacles.

In this contribution, we explore yet another approach which utilizes faunal compositional data on a regional scale. This approach assumes sufficient similarity of taxonomic composition at different studied places, and that common environmental forcing (biotic or abiotic) enables similar temporal changes in community compositions. For this purpose, so-called recurrence plot-based techniques were used, which utilize structures that are apparent in distance matrices for the optimal matching of two sequences. This synchronization approach was successfully tested with moderately successful results on mid- to late Homerian conodonts, utilizing their summed abundance patterns at different geographical locations in the Silurian Baltic Basin (Spiridonov, 2017). Here, the contrast is that compositional data on conodont species diversity are used and new correlation protocols are proposed.

In order to compare species diversity changes in the studied geological sections, we employed two approaches: 1) comparing raw diversities between the samples, and 2) comparing synthetic non-metric multidimensional scaling (NMDS) axes as surrogates for the major compositional gradients. The first approach was a comparison of samples using their species composition using a modified Morisita–Horn similarity index (Horn, 1966), where we assigned barren samples zero similarity. Later on, we converted this similarity measure into the opposite compositional distance measure $d_{ij} = 1 - C_{ij}$, where C_{ij} is the Morisita–Horn similarity between samples i and j (for a further justification of the methodology, see Spiridonov et al., 2017b). The obtained distance matrices were used for calculating the recurrence and cross-recurrence plots. A recurrence plot is a filtered distance matrix, where similar states are coded "1" (the black dots in the diagram) and differing states are coded "0" (the white dots in the diagram). Mathematically, a recurrence plot matrix of compositional distances can be expressed in the following way (Spiridonov et al., 2017b):

$$R_{i,j}(\varepsilon) = \theta(\varepsilon - d_{ij}), for\ i, j = i, ...N \quad (1)$$

Here, R is a recurrence matrix, $\theta(\cdot)$ is the Heaviside step function and ε is the threshold level of similarity. The threshold values (ε) were automatically adjusted so that the studied recurrence plots would have a 20% recurrence rate – an amount sufficient to approximately uniformly (with respect to time) cover the recurrence plots of highly non-stationary and overdispersed time series of conodont abundance.

In the same way, we can compare diversity profiles from two different stratigraphical series (cores), using so-called cross-recurrence plots (Marwan and Kurths, 2002; Marwan et al., 2007; Webber and Marwan, 2015):

$$CR_{i,j}(\varepsilon) = \theta(\varepsilon - d(x_i, y_j)), for\ i = 1, ...N, 1, ...M \quad (2)$$

Here, $CR_{i,\ j}(\varepsilon)$ is a rectangular cross-recurrence matrix comparing two time series of x_i and y_j, which are conodont compositions in two compared samples from two different cores. The structures that appear in the recurrence (and cross-recurrence) matrices can be utilized for studying the system's dynamical features. Horizontal and vertical lines represent unchanging and very similar (so-called "laminar") states (Marwan et al., 2007). Diagonal lines are often called the determinism of a system, which means that a system visits the same portions of state spaces, and is thus attracted to this portion of the total state space. Diagonal lines, or more generally diagonally arranged structures in cross-recurrence plots (as here we are working with geologically distorted signals), are of utmost importance for synchronizing arranged stratigraphical series, since they show that the evolutions of two systems occurred in a similar way in two compared places.

In the second approach, we analyzed conodont compositional variation patterns using a non-metric multidimensional scaling (NMDS) procedure with the Raup–Crick similarity index, which readily handles very different sample sizes (Raup and Crick, 1979). The NMDS procedure was implemented in the PAST (version 3.18) statistical analysis programme (Hammer et al., 2001). This procedure was used in order to reveal the most significant gradients (Kruskal, 1964) in community composition – whether depth or other crucial environmental variables, or possibly the time progression of species changes (Hammer and Harper, 2008; Patzkowsky and Holland, 2012). The NMDS procedure reduces variability to the two or three axes that can serve as new variables whose meaning is interpreted using prior knowledge of the studied ecological communities. The newly obtained NMDS axes were used as an input for the recurrence and cross-recurrence analysis. In this case, instead of simultaneously comparing sample compositions with lots of species (dimensions), the single scalar values of curves were compared. This approach can be seen as an extension and automation of the faunal gradient analysis and resembling approaches, which use similar patterns at different places in the shifts in the biofacies as indicators of the same geological time (for more examples, see Cisne and Rabe, 1978; Foote et al., 2007; Holland et al., 2000; Miller et al., 2001).

Since many productive samples had a low abundance of conodont elements, as was expected, the NMDS analysis with the data revealed a very poor fit (*stress* ≈ 1). Therefore, in order to save a maximal number of data points, and at the same time increase the performance of the non-metric multidimensional scaling procedure, we culled out low abundance samples from the analyzed data until we reached a tolerable misfit level (*stress* < 0.3). This resulted in using samples which had a total abundance of ≥9 conodont elements per sample. This data constraint was satisfied by a total of 206 productive samples from the original 411 productive samples. Species abundance distributions are usually strongly skewed (Gotelli and Graves, 1996; Spiridonov et al., 2017a); therefore, during their multinomial sampling larger sample sizes are often needed in order to gain short-duration taxa (useful for revealing time-related compositional gradients), which in our case, as a rule, are much rarer than long-ranging generalists such as *Panderodus unicostatus*. Later on, for the purpose of creating recurrence plots and time series synchronization, in order to avoid gap distortion in the recurrence analyses, a stratigraphical series of the NMDS1 axis values were interpolated every 1 m in each core. The NMDS1 axis explained a major part of the observed variance – $r_{multiple}{}^2 = 0.55$(highly significant at $p(a) = 0.001$). The significance of NMDS 1 $r_{multiple}{}^2$ was estimated based on the method presented in (Abdi, 2007): the p value for the multiple linear regression determination coefficient can be accessed by knowing the sample size (n = *206* samples) and the number of independent variables or, in this case, the species ($k = 45$), by accessing it with the F-statistic$F = \frac{r^2_{multiple}}{1 - r^2_{multiple}} \times \frac{n - k - 1}{k} = 4.34$, with $\nu_1 = k$ and $\nu_2 = n - k - 1$ degrees of freedom.

The next stage of the analysis was the synchronization itself. Estimating the synchronization (correlation) line is based on similar changes in the biotic composition and the fluctuation patterns that can be traced through a multivariate comparison of compositional differences between samples. Where there is no sedimentological distortion of the primary signal and equal sedimentation rates and biotic changes, we would expect to see a perfect diagonal recurrence line in a cross-recurrence plot and there would be no problem estimating the line of correlation (for examples of this kind of correlation in stratigraphically simple settings, see (Marwan et al., 2002). However, since in general, and especially if we are dealing with the fossil record from different facies and long time scales, we cannot hope that the assumptions of uniform sedimentology and very close biotic turnover would hold. The stratigraphical breaks and variations in sedimentation rates impose distortions on the diagonal structures in recurrence plots that are used for stratigraphical correlation; therefore, monotonous search (i.e., searching for the closest increasing recurrence points in the x and y directions) procedures can be ineffective when searching optimal

correlation paths for stratigraphical sequence alignment. Therefore, in our estimation of correlation lines we employed two techniques that can readily account for nonlinear distortions of primary environmental signals: 1) a traditional dynamical time warping algorithm; 2) and a moving window median recurrence point search algorithm, which is described in this contribution.

Dynamical time warping (DTW) is an iterative numerical algorithm which searches for a minimal path between two points in a distance matrix by incrementally estimating the cost of moving in any given direction by summing the minimal distances of the previous neighbouring comparisons in a distance matrix. The found path can be used for the alignment of two similar sequences which vary nonlinearly in their absolute rates of change. This algorithm has proven its efficiency in aligning strongly varying temporal signals such as music and voice patterns (Müller, 2007). More importantly, it has been successfully applied to the geological correlation of geophysical logs in geologically similar environments, sometimes across significant distances (Hladil et al., 2010, 2011), and even to studying Ludlow successions in the Prague Basin (Chadimova et al., 2015). The current application is a challenging task for this technique, which is advised to be used in situations where there is very dense sampling and a low probability of large hiatuses (Hladil et al., 2010).

The moving window median (MWM) recurrence point search algorithm implementation is based on the analysis of recurrence point distributions in moving windows of predetermined size. The search starts from the origin point, when all the recurring points (black in the matrix) which fall into the rectangular window are ranked and the median position of the observed distribution is estimated for both the x and y directions. In this way, a new correlation point (CP) between two sections is obtained:

$$CP_k^{\tau_x,\tau_y} = \left[Median(x_{ri},\ldots,x_{ri+\tau_x}); Median(y_{rj},\ldots,y_{rj+\tau_y}) \right] \quad (3)$$

Here, τ_x, τ_y are the side lengths of the search windows for the x and y directions accordingly, and x_r and y_r are the recurrent points in the given directions. The search iteratively continues from the newly obtained correlation points by moving the search window in both the x and y directions. If no recurrence points are found in any given window, the next window starts its search from the upper right-most point of the previous window. Therefore, in any given search iteration, correlation points can be either recurrent or non recurrent. The search ends when the last window approaches with its sides in the upper-right-hand corner of the matrix and the ultimate stratigraphic correlation point is estimated.

In order to give equal importance to moving the correlation window in both the x and y directions, the lengths of the sides of the search windows were scaled to 1/5 of the stratigraphical series lengths in the given directions. For example, if the lengths of stratigraphical section x are 100 samples, then the search window's side is set to 20 samples in the corresponding axis; and if stratigraphical section y has lengths of 200 samples, then the side length of the window would be 40 samples in that axis. The larger the size of the search window, the greater the accuracy of the comparison, as the search is more global. On the other hand, increasing the size of the search window decreases precision, as fewer correlation points can be estimated and used for correlating two geological records. Therefore, it is advisable to guide the choice of window size based on prior knowledge of macrofacies. Monotonous deep-water succession will most likely benefit from smaller search windows. On the other hand, near shore and very non-stationary sequences with more disrupted patterns, as those presented here, should be studied using larger search windows.

Interpolating the diversity data was performed in an R computational environment (R Development Core Team, 2015). The recurrence and cross-recurrence plot calculation and visualization (partially based on those presented in Spiridonov et al., 2017b), as well as the synchronization procedures, were performed using custom-made scripts in the *Perl* environment.

4. Results

4.1. Integrated stratigraphy

In this contribution, Viduklė-61 was chosen as a reference section for all the comparative analyses, due to its detailed level of study throughout the entire Wenlock and Ludlow interval (Martma et al., 2005; Radzevičius et al., 2014a, 2017; Venckutė-Aleksienė et al., 2016), although, other sections (especially Gėluva-99 and Gėluva-118) have substantially higher average abundances of conodont elements per sample. This is probably due to their proximity to the shoreline as well as and fact that the succession preserved at these localities is the Ludlow interval only. The Milaičiai-103 core was studied in a similar level of detail, although shorter interval – the middle and upper parts of the Ludlow was researched (Spiridonov et al., 2017b). As it was described previously (Spiridonov et al., 2017b), its detailed integrated stratigraphy will not be discussed here. The new and refined data on the conodont distributions in the Vuduklė-61 core, together with the $\delta^{13}C_{carb}$ data, allow international zones to be established in the studied portion of the section.

In this contribution, we have followed the zonation and integrated stratigraphical framework for the Silurian as proposed in the Geological Time Scale 2012 (Melchin et al., 2012), but with some differences in the Gorstian and lowermost Ludfordian zonation (see below for details). The conodont zones were determined by the presence of index taxa and accompanying time-restricted faunas. In addition, the exact placement of the zonal boundaries, if necessary due to the rarity of time-specific conodont material, was specified based on additional graptolite, chemostratigraphical, lithological and gamma ray log material. For reference, in the summary illustration we also placed international conodont zones next to the operational zones used in this contribution.

The lower part of the section has very sparse conodont remains (Fig. 2), although the time restricted taxa were identified in the previous study (*Ozarkodina bohemica longa*, *Kockelella ortus absidata*) and it was unambiguously proven that the double-peaked $\delta^{13}C_{carb}$ excursion in the Wenlock is the Mulde Excursion. The shape of the $\delta^{13}C_{carb}$ curve and the identity of the conodont species, as well as abundant graptolite material (Radzevičius et al., 2014a), suggest that the lowermost interval belongs to the *Ozarkodina bohemica longa* Zone up to a depth interval of approximately 1290 m, where the *Kockelella ortus absidata* Interval Zone begins. The *Kockelella ortus absidata* Interval Zone ends at a depth of approximately 1275 m. The earliest Ludlow zonal species *Kockelella crassa* was not recovered in the studied section; therefore, the entire Gorstian age and probably part of the lowest Ludfordian was assigned to the *Kockelella variabilis* Interval Zone (Corradini and Serpagli, 1999; Corriga et al., 2009), which ends at a depth of 1179.9 m. At this level, the *Polygnathoides siluricus* Zone starts, and it ends at a depth of 1160.6 m. The *K. variabilis* Interval Zone accounts for a wider stratigraphical interval than is used in most other contributions (e.g. Melchin et al., 2012) and subsumes the *K. crassa* Zone and *Ancoradella ploeckensis* Zone, which were also unrecognized in the current material due to the absence of the index taxa, most probably because of ecological or biogeographical factors, or simply because of their rarity. The *Polygnathoides siluricus* Zone is inferred at the same depth as the last appearance of the *Kockelella* genus, 1158.6 m, as this genus, is known to disappear prior to the last appearances of *Polygnathoides siluricus* in the wide range of records (Slavik et al., 2010; Corriga et al., 2014; Corradini et al., 2015; Schönlaub et al., 2017). The next interval is typified by conodonts that are characteristic for the post-Lau Event survival fauna (Jeppsson et al., 2012). A very high abundance *Panderodus equicostatus* “time anomalous” (Spiridonov et al., 2017b) interval with rare finds of zonal *Ozarkodina snajdri* species can be found. Based on the distribution of the discussed species and the features of the

$\delta^{13}C_{carb}$ curve, the boundaries of the *Ozarkodina snajdri* Interval Zone can be drawn between 1160.6 and 1112.7 m. From this point on, the *Ozarkodina baccata-Ozarkodina crispa* Zone (Miller and Aldridge, 1997; Radzevičius et al., 2016; Spiridonov et al., 2017b) can be distinguished in the interval between 1112.7 and 1089.7 m.

The Gėluva-99 core section from the fore-shore facies zone represents a relatively distinct set of conodonts from those found in the Viduklė-61 and Milaičiai-103 cores (Fig. 3). However, some time-specific taxa, as well as the $\delta^{13}C_{carb}$ and natural gamma logs, show a clear stratigraphical signal. There are several of *Ozarkodina bohemica longa* and *Panderodus equicostatus* in the lower portion of the section, which is also associated with trend of decreasing stable carbon isotope values from close to $\delta^{13}C_{carb} = +1‰$. This observation points to the conclusion that this is the end of the second peak of the Mulde Excursion. A very similar association of taxa and stable isotopic changes were detected in the shallow water succession of the Ledai-179 section (Radzevičius et al., 2014b). A combination of these features allows us to distinguish a chronostratigraphic analogue of the *Kockelella ortus absidata* Interval Zone at a depth interval between 858.9 and 812 m. The depth interval between 812 and 750.4 m is typified by an assemblage of conodont taxa that are usual for the early Gorstian such as *Ozarkodina bohemica bohemica*, *Ctenognathodus* sp. *S.* and *Ozarkodina anika* (Fig. 5) (Viira and Einasto, 2003; Radzevičius et al., 2014b). Therefore, based on these observations, the given depth interval can putatively be assigned to the *Kockelella variabilis* generalized Interval Zone. The uppermost studied sample in this section, at a depth of 750.2 m, can be unambiguously assigned to the *Ozarkodina baccata – Ozarkodina crispa* Zone of the uppermost Ludlow.

The Gėluva-118 core data are the most informationally restricted dataset studied in this contribution. The geophysical logs were not recorded during the drilling of this core, and there are very few stratigraphically short-lived taxa in the lower portion of the section (Fig. 4). On the other hand, a combination of the $\delta^{13}C_{carb}$ and conodont data, as well as a comparison with the geographically close core section make the age inference plausible. The presence of *Kockelella ortus absidata* in association with the descending limb of the $\delta^{13}C_{carb}$ excursion in the lower and middle parts of the section indicate that it is the second peak of the Mulde Excursion. Based on this observation and on the matching shapes of the $\delta^{13}C_{carb}$ curves in this section, as well as in the Gėluva-99 and Viduklė-61 sections, the *Kockelella ortus absidata* Interval Zone in this section is suggested to stretch from 1006.6 m up to approximately 930 m. Appearances of *Wurmiella inflata* with a form similar to *Ozarkodina soegina* (*Ozarkodina* aff. *soegina*) suggest that in the middle part of the studied section, there is a Gorstian conodont fauna (Viira and Einasto, 2003; Corriga et al., 2009; Radzevičius et al., 2016; Spiridonov et al., 2017b). Based on this evidence, the interval between 930 and 859.3 m can be assigned to the *Kockelella variabilis* generalized Interval Zone. On the other hand, the portion of the section between 859.3 and 847.3 m can be unambiguously attributed to the *Ozarkodina baccata – Ozarkodina crispa* Zone of the uppermost Ludfordian, as both species are found in close association in most of the samples.

4.2. Stratigraphic patterns of conodont community turnover

The recurrence plot analyses (Fig. 6) revealed conodont community evolution patterns which are congruent with the integrated stratigraphical analysis results. The Viduklė-61 core section (Fig. 6A) shows recurrence patterns which are very similar to those exhibited by the Milaičiai-103 core section (Fig. 6B). A highly recurrent (compositionally stable) late Homerian to Gorstian community state is suddenly replaced by a very time-specific ("time anomalous"), (Spiridonov et al., 2017b) state at a depth of 1152.5 m in the aftermath of the Lau Event, where the disaster taxon *Panderodus equicostatus* dominates assemblages in the *Ozarkodina snajdri* Interval Zone. A visual comparison of these two cores demonstrates their stunning similarity. On the other hand, as is expected, no such feature can be detected in either the Gėluva-99 or Gėluva-118 core section recurrence plots of conodont communities (Fig. 6C, D). This observation implies the existence of a significant stratigraphical hiatus in both sections.

A comparison of stratigraphically equivalent portions of sections on the cross-recurrence plots of conodont diversity data (which are based on the Morisita–Horn distance matrices) also reveals patterns that are congruent with the conclusion of the integrated stratigraphy (Fig. 7). The cross-recurrence plots of the Viduklė-61 and Milaičiai-103 conodont communities in the upper Gorstian to Ludlow interval show very close similarity in their recurrence patterns (Fig. 7A, B). Synchronization procedures using both the DTW and MWM approaches show an almost linear correlation line between these two sections. An exception is the DTW and MWM correlation lines, apparently implying some condensation in the lower part of the Viduklė-61 section. A very different situation can be seen in comparisons of the Viduklė-61 section with the Gėluva-99 (Fig. 7C, D) and Gėluva-118 (Fig. 7E, F) sections. An apparent lack of cross-recurrence in the *Ozarkodina snajdri* Interval Zone suggests an absence of this chronostratigraphical unit in both the Gėluva-99 and Gėluva-118 sections. The correlation lines using both approaches (DTW and MWM) correctly assume a sigmoid form. Apparently, the MWM picks a signal more accurately than the DTW algorithm. In the latter case, the inferred condensation horizon should be (based on the integrated stratigraphy) higher in both the Gėluva-99 and Gėluva-118 sections than can be observed in automatically generated correlation lines.

Another approach using a temporal ordering analysis of NMDS1 scores revealed a clearly distinguishable stratigraphical pattern (Fig. 8). There is a state shift in the community composition to higher NMDS1 values at the beginning of the *Ozarkodina snajdri* Interval Zone. At its best, it can be observed in the Viduklė-61 and Milaičiai-103 cores (Fig. 8A, B). This state shift is approximately coincident with the onset of the Lau Event in both cores (Martma et al., 2005; Spiridonov et al., 2017b). The Lau Event as originally defined starts slightly earlier in the upper part of the *Polygnathoides siluricus* Zone and reaches its peak in the lower part of the *Ozarkodina snajdri* Interval Zone, or as defined in some sources in the Icriodontid Zone (Jeppsson et al., 2012). However, as is inferred using the integrated stratigraphical approach, the preserved upper Ludlow part is much smaller in the Gėluva-99 and Gėluva-118, and the state shift is clearly distinguishable in both sections (Fig. 8C, D).

The cross-recurrence plots between the Viduklė-61 and Milaičiai-103 cores show a distinct co-recurring state shift at the onset of the Lau Event (Fig. 9A, B) at 1252.2 m in the Viduklė-61 core and at 1234 m in the Milaičiai-103 core at the onset of the *Ozarkodina snajdri* Interval Zone. Both the DTW and MWM algorithms show that diversity changes in both sections proceeded in a very similar manner. The MWM approach suggests that the correlation line between them should be almost straight, and the DTW shows a more fluctuating pattern, which could be partially related to the frequent occurrence of laminar (compositionally stable) states, which appear as horizontal and vertical structures on the graphs. As in the recurrence plots of the primary diversity data (which are based on the Morisita–Horn distances), there is a distinct lack of recurrence in the *Ozarkodina snajdri* Interval Zone between the Viduklė-61 section and the Gėluva-99 and Gėluva-118 core sections (Fig. 9C, D, F, G). The described observation implies the occurrence of condensation or a significant hiatus. The stratigraphical hiatus, which is probably related to the mid-Ludlow unconformity (Radzevičius et al., 2016) in the Gėluva-99 and Gėluva-118 cores, was spotted by both synchronization techniques (both DTW and MWM) almost ideally. Overall, the cross-recurrence plot analyses of the NMDS1 scores (Fig. 9) revealed correlation patterns that are even more congruent with the integrated stratigraphical model than the cross-recurrence plots, which used conodont diversity data directly (Fig. 7). This may be evidenced by comparing how the correlation paths compare with the Ludlow (as all of its zones are present in every studied section) conodont zone boundaries in the same cores by calculating the

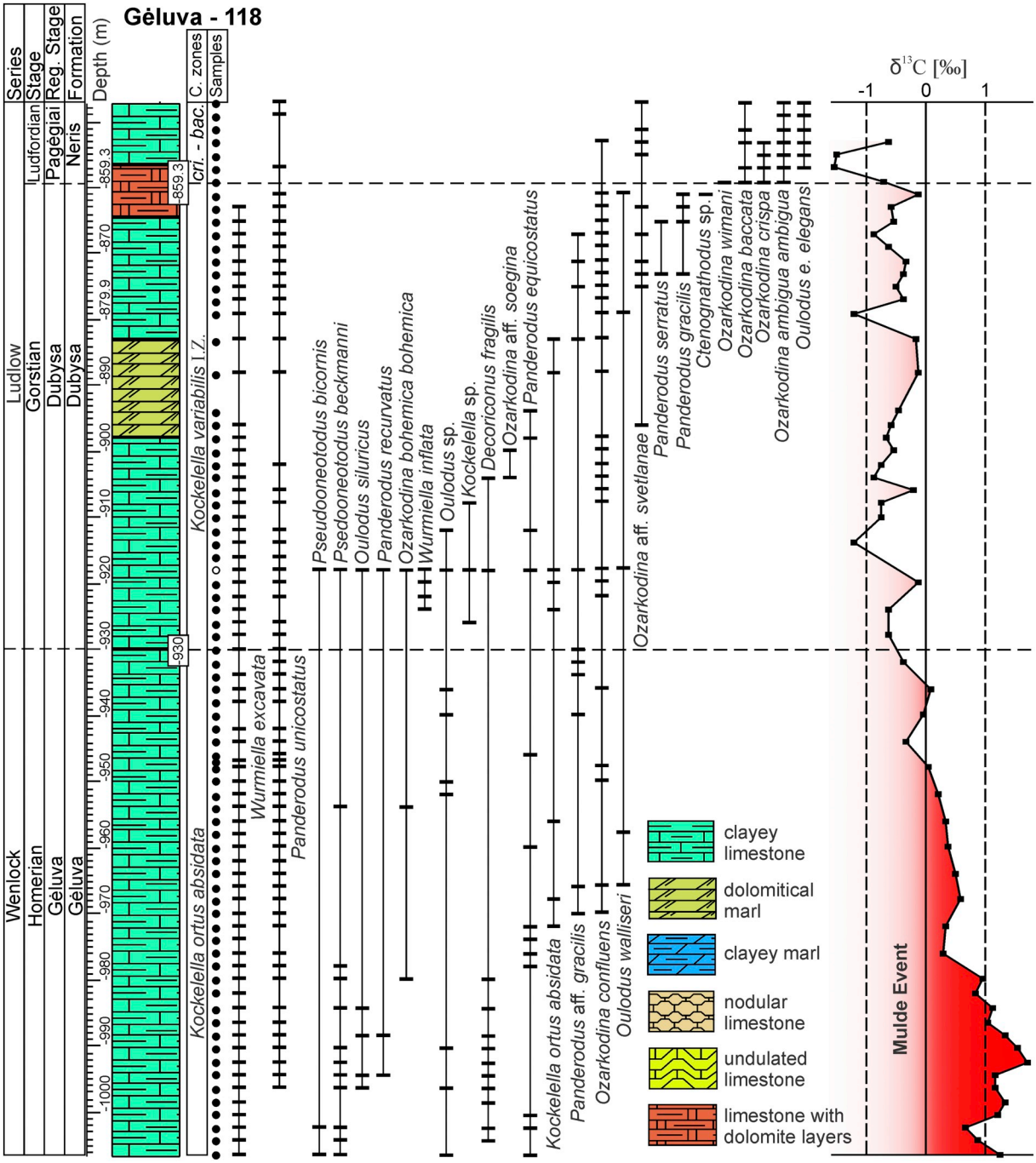

Fig. 4. Stratigraphical scheme for the upper Homerian and Ludlow of the Gėluva-118 core. From left to right: chronostratigraphic and lithostratigraphic subdivisions; lithology; conodont distribution; and $\delta^{13}C$ curve.

average difference on the *y*-axis of the cross-recurrence plots for every approach combination with different correlation methods and data treatments (Table 1). It can be clearly seen that the cross-recurrence synchronization based on raw data was much poorer than the cross-recurrence synchronization based on the NMDS1 scores. In the latter case, the DTW performed on average 1.52 times better, and the MWM 1.39 times better. It should be noted that the overall performances of both methods (classical dynamical time warping versus our proposed moving window median) are very similar (compare the grand averages in Table 1). However, the MWM method shows slightly better average results than the DTW in both cases of using raw data and NMDS1 scores. It should also be mentioned that the boundaries of the conodont zones were determined through the expert judgement of conodont ranges and other supplementary data (gamma ray logs, stable carbon isotopic trends etc.) and, therefore, are hypotheses themselves. Thus, part of the variance between the automatic correlation lines and the zone boundaries should also be attributed to the possible (and probable) inaccuracies in the judgement given the complexity of real world data.

5. Discussion

The stratigraphical patterns of conodont distribution, as revealed by an analysis of the stratigraphical ranges of the zonal taxa in the Viduklė-61 and Milaičiai-103 cores, are highly congruent with the stratigraphical correlation based on the matching features in the $\delta^{13}C_{carb}$ trends (Martma et al., 2005; Radzevičius et al., 2016). The Gorstian

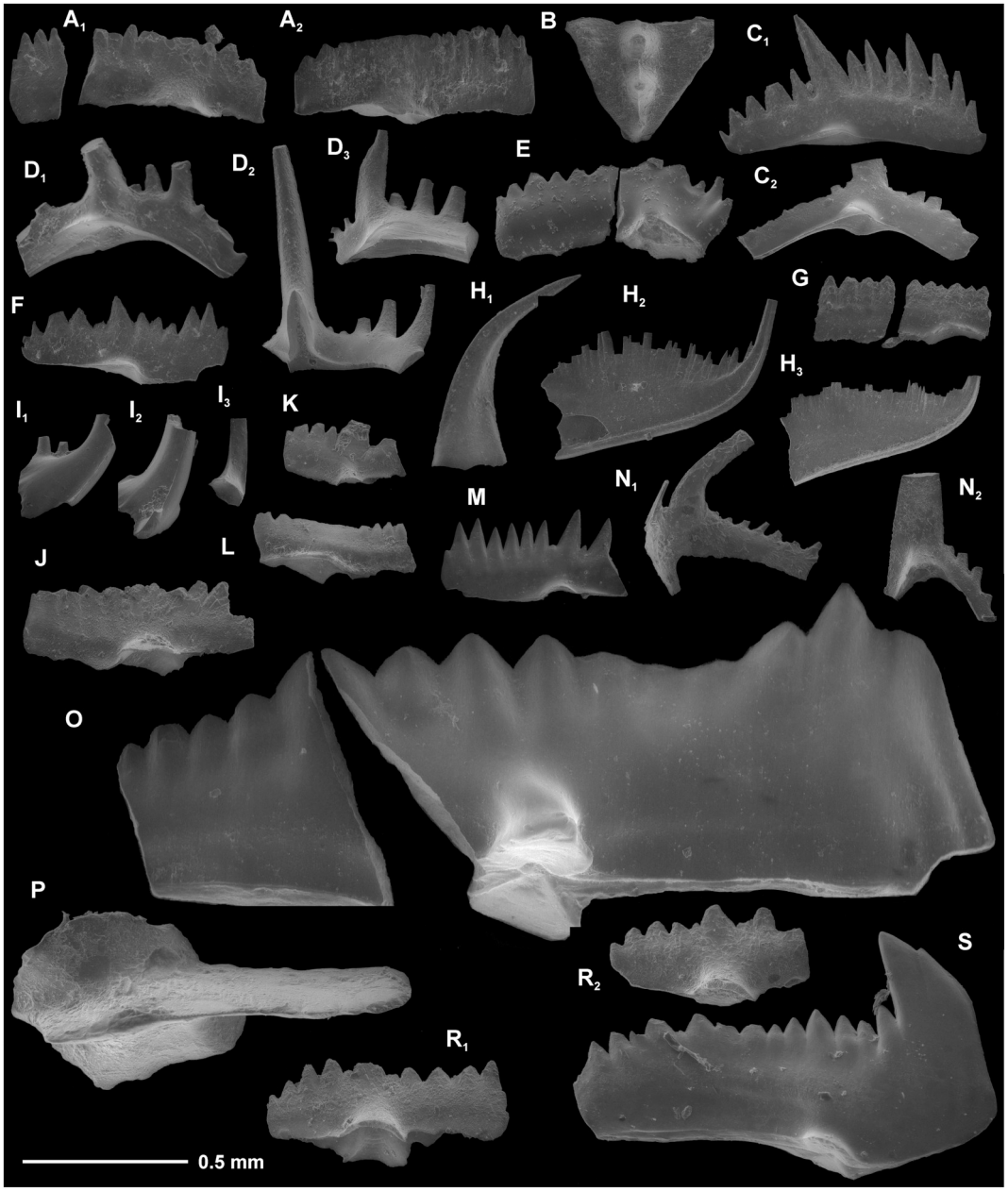

Fig. 5. Scanning electron microscope mircrographs of some stratigraphically important conodonts from the Viduklė-61, Gėluva-99 and Gėluva-118 cores. **A**) *Ozarkodina bohemica bohemica*, Pa elements, Gėluva-99 well, depth 806 m, **A1**) no. VU-CON-GEL99-008, A2) no. VU-CON-GEL99-009. **B**) *Polygnathoides siluricus*, Pa element, no. VU-CON-VID61-013Viduklė-61 well, depth 1179.9 m. **C**) *Wurmiella excavata*, Viduklė-61 well, depth 1162.9, **C1**) Pa element, no. VU-CON-VID61–001, **C2**) Pb element, no. VU-CON-VID61-002. **D**) *Oulodus walliseri*, Gėluva-99 well, depth 801.1 m, **D1**) Pb element, no. VU-CON-GEL99-002, **D2**) Sa element, no. VU-CON-GEL99-003, **D3**) M element, VU-CON-GEL99-004. **E**) *Kockelella ortus absidata*, Pa element, no. VU-CON-GEL118-004, Gėluva-118 well, depth 956.1 m. **F**) *Ozarkodina confluens*, Pa element, no. VU-CON-GEL99-007, Gėluva-99 well, depth 759.4 m. **G**) *Wurmiella inflata*, Pa element, no. VU-CON-GEL118-003, Gėluva-118 well, depth 920.1 m. **H**) *Belodella* sp., Viduklė-61 well, depth 1162.9 m, **H1**) M element, no. VU-CON-VID61-007, **H2**) Sa element, no. VU-CON-VID61-005, **H3**) Sb element, no. VU-CON-VID61-006. **I**) *Coryssognathus dubius*, Viduklė-61 well, depth 1161.8 m, **I1**) Sc element, no. VU-CON-VID61-009, **I2**) Sa element, no. VU-CON-VID61-008, **I3**) Pb element, no. VU-CON-VID61-010. **J**) *Ozarkodina scanica*, Pa element, no. VU-CON-VID61-016, Viduklė-61 well, depth 1127.4 m. **K**) *Ozarkodina wimani*, Pa element, no. VU-CON-VID61-014, Viduklė-61 well, depth 1127.4 m. **L**) *Ozarkodina snajdri*, Pa element, no. VU-CON-VID61-015, Viduklė-61 well, depth 1117.0 m. **M**) *Ozarkodina anika*, Pa element, no. VU-CON-GEL99-001 Gėluva-99 well, depth 764.5 m. **N**) *Oulodus elegans elegans*, Viduklė-61 well, depth 1091.7 m, **N1**) Sc element, no. VU-CON-VID61-003, **N2**) M element, no. VU-CON-VID61-004. **O**) *Ozarkodina svetlanae*, Pa element, no. VU-CON-GEL118-001, Gėluva-118 core, depth 847.3 m. **P**) *Ozarkodina crispa*, Pa element, no. VU-CON-VID61-011, Viduklė-61 well, depth 1073.0 m. **R**) *Ozarkodina baccata*, **R1**) Pa element, no. VU-CON-GEL118-002, Gėluva-118 core, depth 853.3 m, **R2**) Pa element no. VU-CON-GEL99-005, Gėluva-99 core, depth 743.7 m. **S**) *Ozarkodina nasuta*, Pa element, no. VU-CON-VID61-012, Viduklė-61 well, depth 1092.8 m.

Stage in both sections can be unambiguously assigned just at the resolution of the generalized *Kockelella variabilis* Interval Zone. The *Polygnathoides siluricus* Zone can be distinguished in both sections in the rising limb of the Lau Excursion. This is succeeded by the interval of peak and ultimately decreasing trend in the $\delta^{13}C_{carb}$ values. This stratigraphical interval in both cores is typified by the dominance of *Panderodus equicostatus*, which marks compositionally very distinct "time anomalous" conodont communities, as well as compositionally very distinct brachiopod communities in Baltica (Spiridonov et al., 2017b), and possibly other shelly taxa in Bohemia as well (Manda and

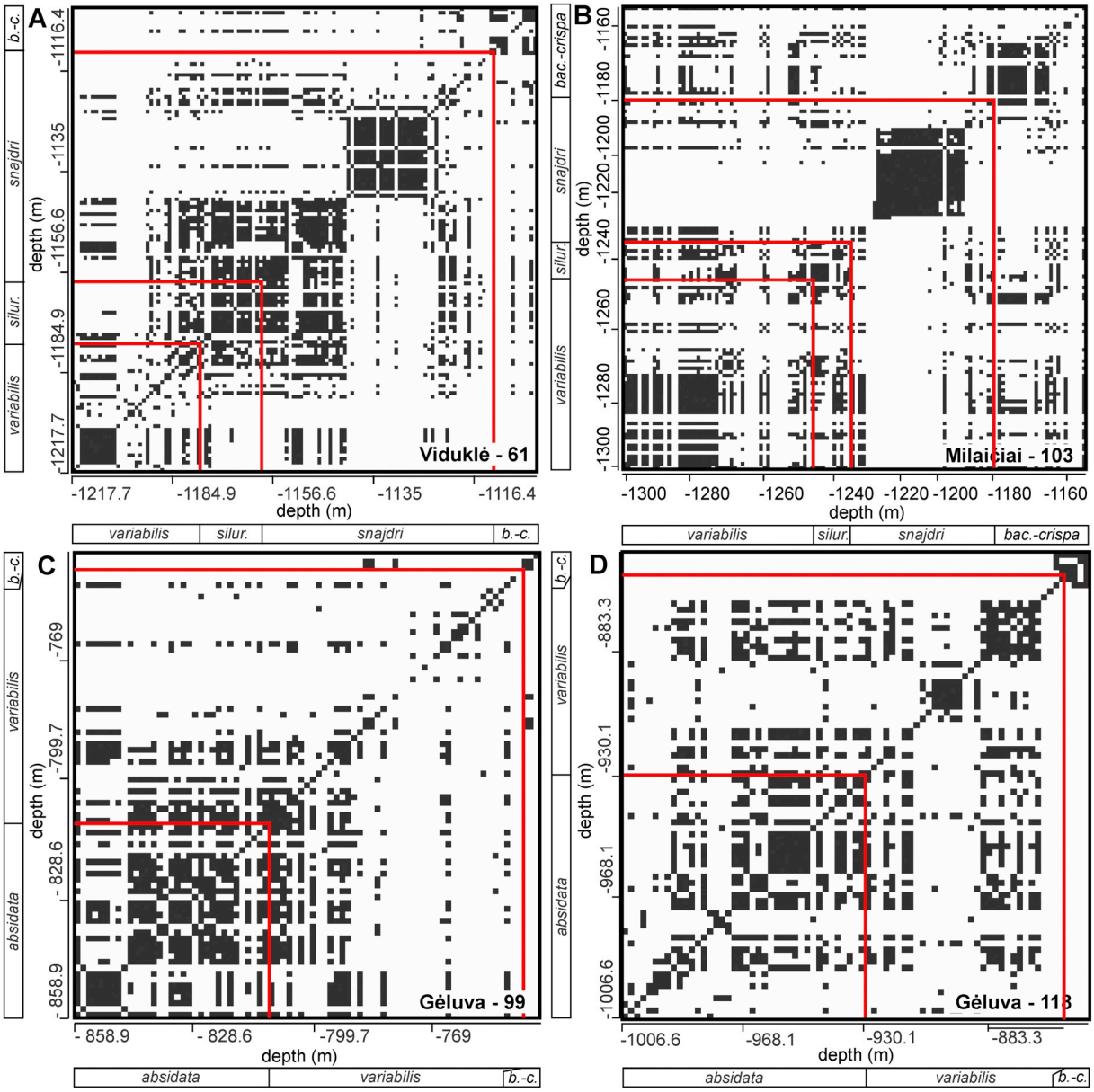

Fig. 6. Recurrence (autorecurrence) plots of conodont diversity comparisons (based on the Morisita–Horn similarity index) from the studied sections: a) Viduklė-61 core; b) Milaičiai-103 core (Spiridonov et al., 2017b); c) Gėluva-99; d) Gėluva-118. The conodont zones are indicated by the dashed lines.

Frýda, 2014). The same stratigraphical levels, as shown previously, coincided with an anachronistic reappearance of (abundant) stromatolites in near shore environments (Calner, 2005; Radzevičius et al., 2016). In the upper parts of the section the *Ozarkodina baccata- Ozarkodina crispa* Zone can be distinguished, as both appeared in the studied sections during the interval just after the end of the Ludfordian Lau Excursion and mark the uppermost Ludlow part of the succession. A very similar pattern of succession, with an association of *Ozarkodina baccata* and *Ozarkodina crispa*, as well as other taxa with long durations (i.e., *Wurmiella excavata* and *Panderodus unicostatus*), can be observed in the Bohemia sections (Slavik et al., 2010; Slavik and Carls, 2012).

The Gėluva-118 and Gėluva-99 sections in their lower parts can be correlated with the contemporaneous records of the Ledai-179 and Vilkaviškis-134 sections according to the similarity of their fauna and the distinct protracted falling limb of the second peak of the Mulde Excursion (Radzevičius et al., 2014b, 2016). This points to the presence of upper Homerian strata in both of these sections. Some temporally restricted (Viira and Einasto, 2003; Radzevičius et al., 2014b) taxa such as *Ctenognathodus* sp. S and *Ozarkodina* aff. *soegina*, as well as *Ozarkodina anika*, suggest the preservation of the Gorstian strata in these two sections. The lack of the distinctive mid-Ludfordian $\delta^{13}C_{carb}$ anomaly in the Gėluva-118 and Gėluva-99, as well as a lack of time-specific conodont taxa from the lower and middle parts of the Ludfordian suggest that there is significant disconformity in these more proximal sections. The presence of this significant disconformity, which spans most of the Ludfordian and probably part of the Gorstian, is also suggested by the cross-recurrence comparisons of the Viduklė-61 section with the Gėluva-118 and Gėluva-99 sections, which were based on the diversity and turnover metrics of conodont communities. The retreat of the basin, interpreted from the present material and the paleogeographical reconstructions (Einasto et al., 1986; Lazauskienė et al., 2003), suggest a very large regression with a horizontal seaward shift of the shoreline by >100 km in the Lithuanian part of the Silurian Baltic Basin during Ludfordian time (see summary Fig. 10). The absence of the lower part of the Lau Event recorded in Bohemia, which is explained by the influence of local factors (Slavik et al., 2010), can be also explained by the

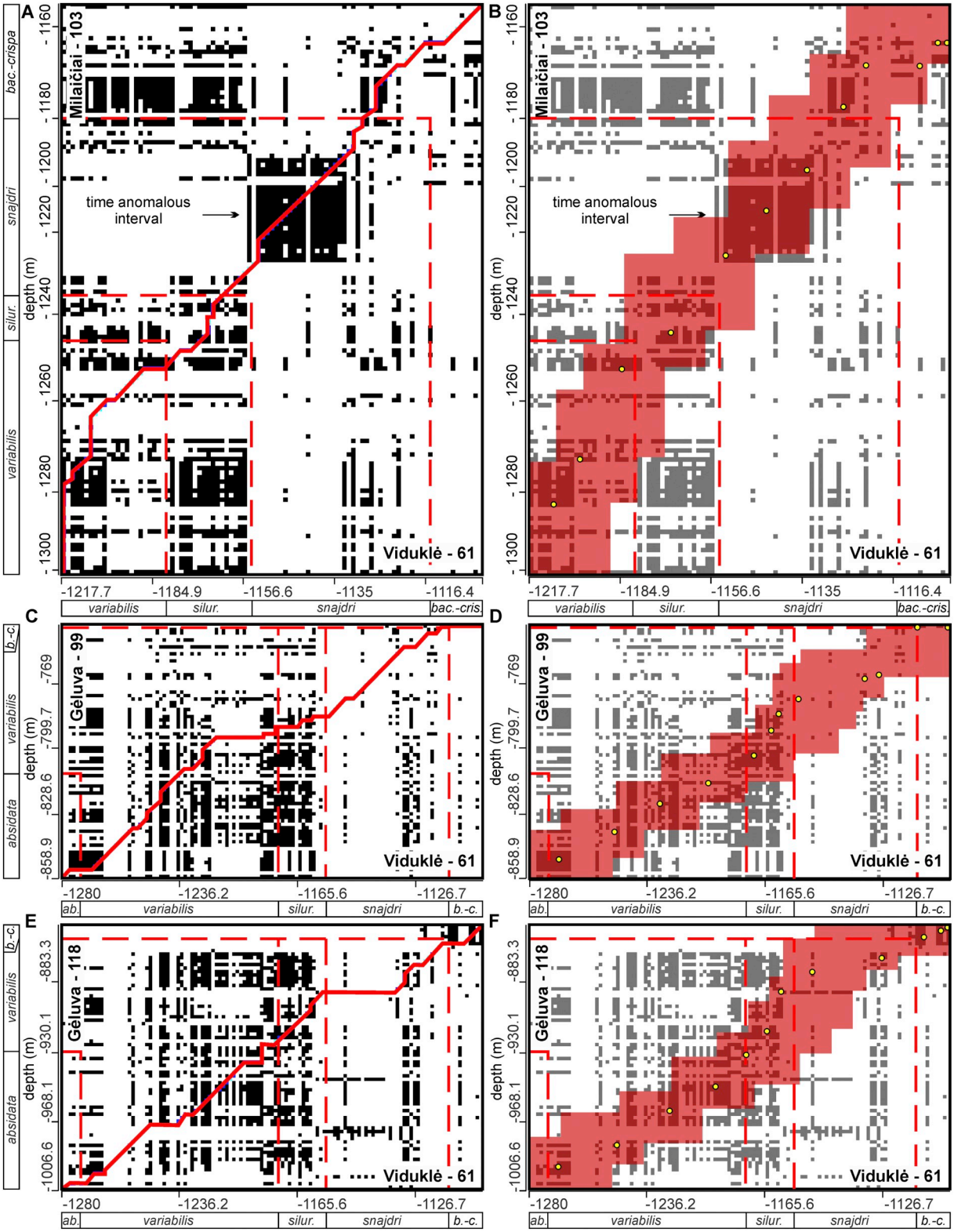

Fig. 7. Cross-recurrence plots of diversity data (based on the Morisita–Horn similarity index) with estimated synchronization (stratigraphical correlation) paths: A) and B) Viduklė-61 and Milaičiai-61 cores; C) and D) Viduklė-61 and Gėluva-99 cores; E) and F) Viduklė-61 and Gėluva-118 cores. The right-hand column (A, C, E) shows the synchronization performed using the dynamical time warping algorithm. The left-hand column (B, D, F) shows the synchronization performed using the moving window median recurrence point search algorithm. The red rectangles show the median search windows and the highlighted points are the correlation (synchronization) points. The conodont zones are indicated by the dashed lines. (For interpretation of the references to colour in this figure legend, the reader is referred to the web version of this article.)

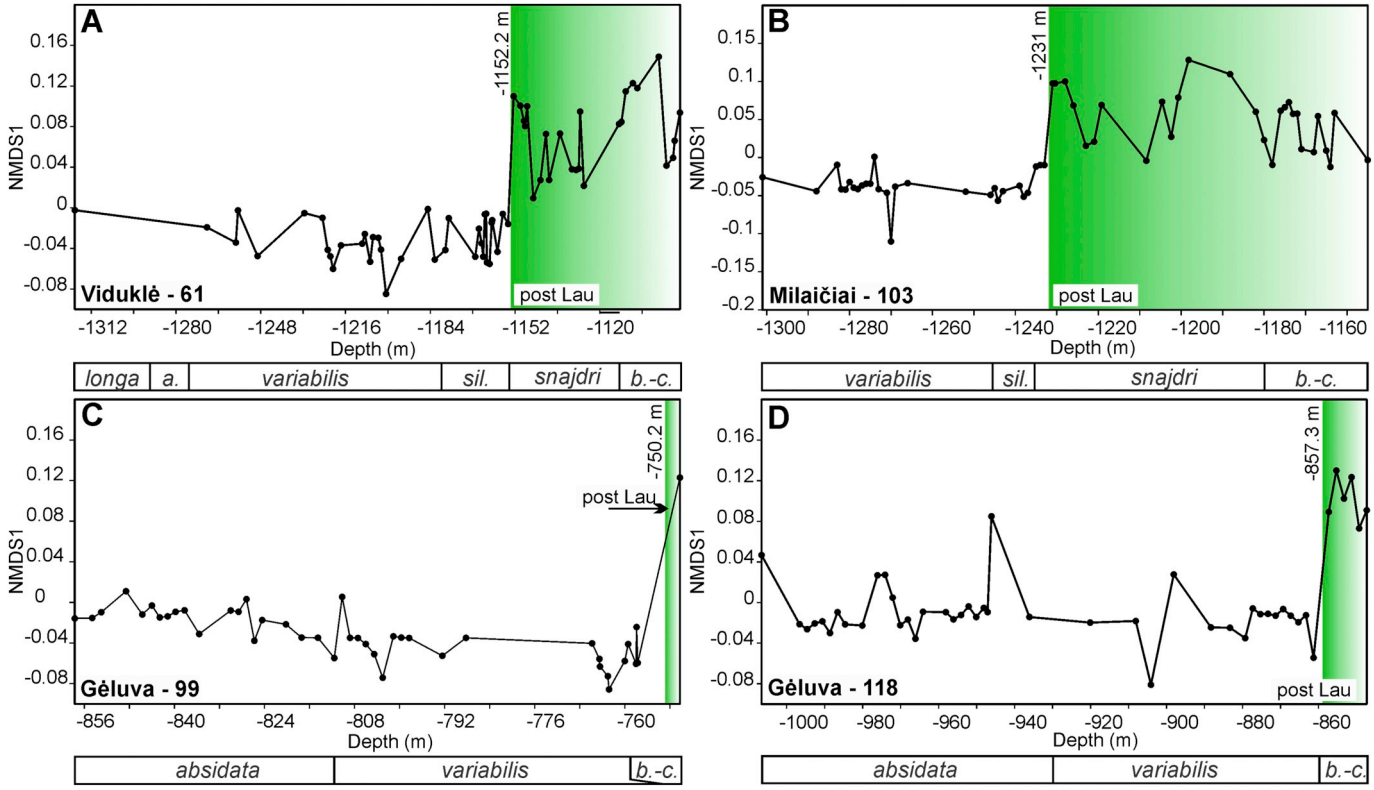

Fig. 8. Plots of the NMDS1 axis scores for conodont communities as a function of core depths: A) Viduklė-61; B) Milaičiai-103; C) Gėluva-99; D) Gėluva-118.

eustatic sea level drop pulse in the vicinity of this event, or possibly more pulses based on the stable oxygen isotopic estimates of sea water temperature changes (Lehnert et al., 2007a; Trotter et al., 2016).

An inspection of the recurrence and cross-recurrence plots shows that the Lau Event, which is associated with the end of the *Polygnathoides siluricus* Zone (Jeppsson, 1998; Jeppsson and Aldridge, 2000; Jeppsson et al., 2012), was the only significant event during this interval of the Silurian to have a lasting impact on conodont communities. Its immediate aftermath was associated with the development of compositionally anomalous communities (Spiridonov et al., 2017b) strongly dominated by *Panderodus equicostatus*, which can be detected in the offshore section in Lithuania, as well as in Gotland (Jeppsson, 1998), which did not experience the erosional episodes related to the climatic pulses of the mid-Ludfordian (Calner and Eriksson, 2006; Lehnert et al., 2007a). This pattern can be most clearly seen in the time series of the NMDS1 scores for the ordinated Homerian to Ludlow conodont communities from the Silurian Baltic Basin and their recurrence plots for the Milaičiai-103 and Viduklė-61 cores (Fig. 8A, B). The entire Mulde interval (mid- to late Homerian), the entire Gorstian time and the beginning of the Ludfordian were marked by relatively stable community compositions, as can be seen from the high cross-recurrence rates in this stratigraphical interval. The precise role and effects of the Mulde Event cannot be accessed in the current data because there are too few data points from the interval before the onset of the perturbation. On the other hand, the communities that lived immediately after the Mulde extinction episode were very similar to those that persisted up until the Lau Event. This suggests that any events that might have occurred between the late Homerian and early Ludfordian time (such as the earliest Ludfordian Linde Event (Jeppsson, 1998; Jeppsson, 2005)) were of relatively minor importance for conodont community changes.

It is interesting that a very sharp transition to higher NMDS1 values occurred at the base of the *Ozarkodina snajdri* Interval Zone. The new state was much less stable, as can be seen from the lower recurrence rates – a sparser appearance of the sub-matrix (upper-right-hand portions of the cross-recurrence plots in Fig. 9A, B). The same transition can be seen in the much less complete Gėluva-99 and Gėluva-118 deep core sections (Fig. 8C, D). As it happens, this is a very useful feature that can be utilized for the high resolution correlation of strata using cross-recurrence plots (Fig. 9C–F). The previously described compositional transition can be characterized as a community state shift, which is usually accompanied by alterations in the functional dynamics of ecosystems (Scheffer and Carpenter, 2003; Sirota et al., 2013; Roopnarine and Angielczyk, 2015; Spiridonov et al., 2016). These kinds of transitions are expected and were described during the aftermaths of profound mass extinctions such as the “Great Dying” of the P-Tr (Dineen et al., 2014; Hull et al., 2015), the Tr-J episode of sudden environmental changes (Ritterbush et al., 2015a; Ritterbush et al., 2015b) or the K-Pg extinction event (Aberhan and Kiessling, 2015). The Lau Event was of exceptional importance in the context of Silurian episodes and events, affecting the compositional patterns of other (non-conodont) vertebrate communities, with major losses in the dominant clades (Eriksson et al., 2009). Therefore, the current contribution demonstrates rapid pace, significant magnitude, geographical spread and the persistence of the effects of the Lau Event on the conodont fauna in the Baltic region.

The spatially and temporally coherent response of the conodont communities, as evidenced by the recurrence and cross-recurrence plots (using both primary diversity data and NMDS1 axis scores), enabled a high resolution correlation of the sections in the eastern part of the Silurian Baltic Basin even with no significant input from other sources of information. Only the beginnings and endings of the studied records should be approximately matched based on other sources of stratigraphical evidence. This will increase the accuracy of comparison, but it is not a prerequisite. However, sharply differing borderline stratigraphical regions would be matched less accurately. In terms of future developments, it could be envisioned that shorter sequences with enough spatial and temporal coherence could be matched with longer sequences in a manner similar to searching for homologous genes in DNA sequences of widely differing lengths.

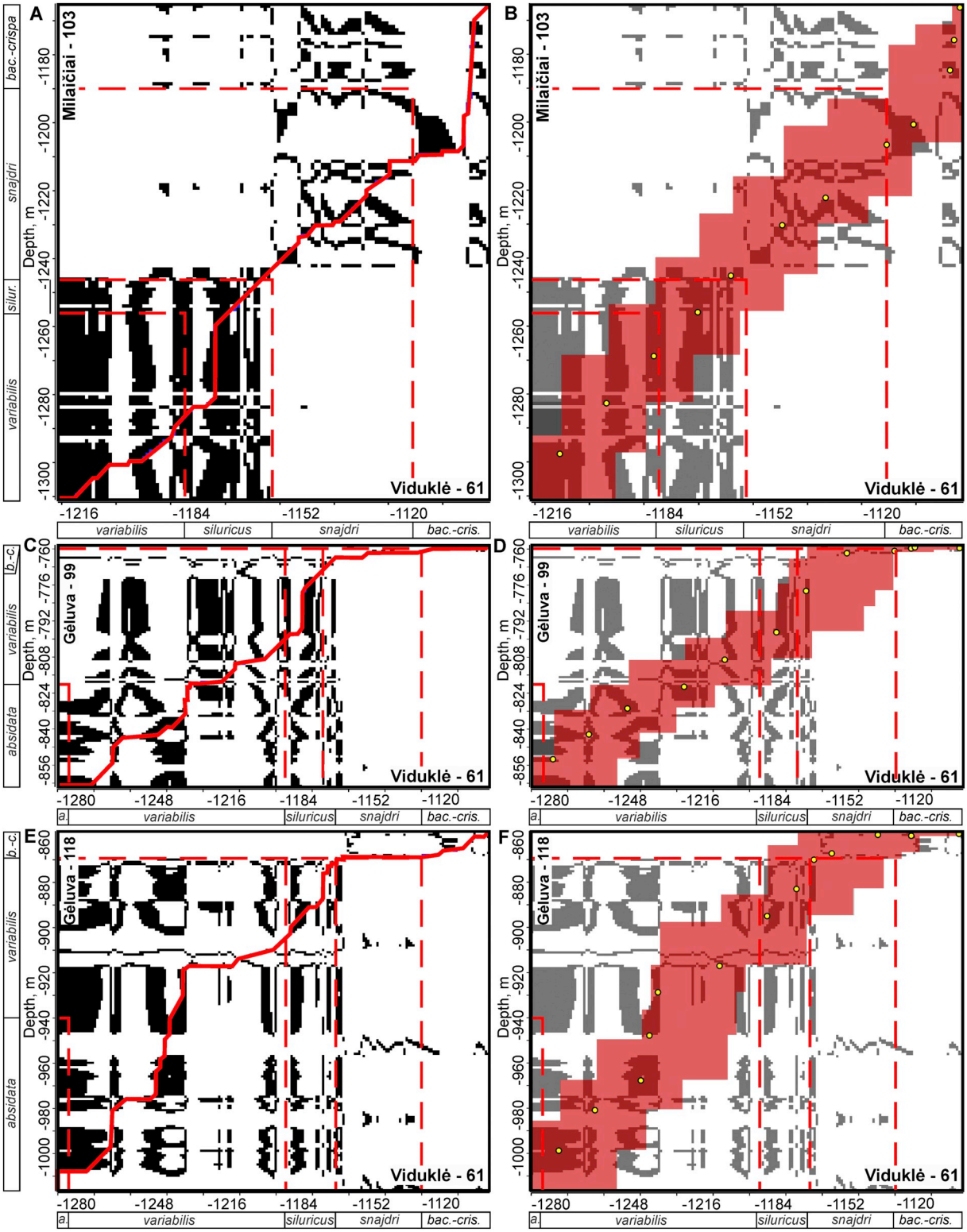

Fig. 9. Cross-recurrence plots of conodont diversity data, based on the comparisons of the stratigraphically arranged and interpolated NMDS1 scores of conodont community compositions, together with the estimated synchronization paths: A) and B) Viduklė-61 and Milaičiai-61 cores; C) and D) Viduklė-61 and Gėluva-99 cores; E) and F) Viduklė-61 and Gėluva-118 cores. The right-hand column (A, C, E) shows the synchronization performed using the dynamical time warping algorithm. The left-hand column (B, D, F) shows the synchronization performed using the moving window median recurrence point search algorithm. The red rectangles show the median search windows and the highlighted points are the correlation (synchronization) points. The conodont zones are indicated by the dashed lines. (For interpretation of the references to colour in this figure legend, the reader is referred to the web version of this article.)

Even though all of the cross-recurrence plot analyses (using DTW and MWM) revealed the most significant stratigraphical features (mid-Ludlow unconformity), the analyses which utilized the NMDS1 scores based on the analysis of the reduced data were the most accurate. This observation indicates possible ways of improving cross-recurrence plot-based diversity analyses and stratigraphical correlations which are

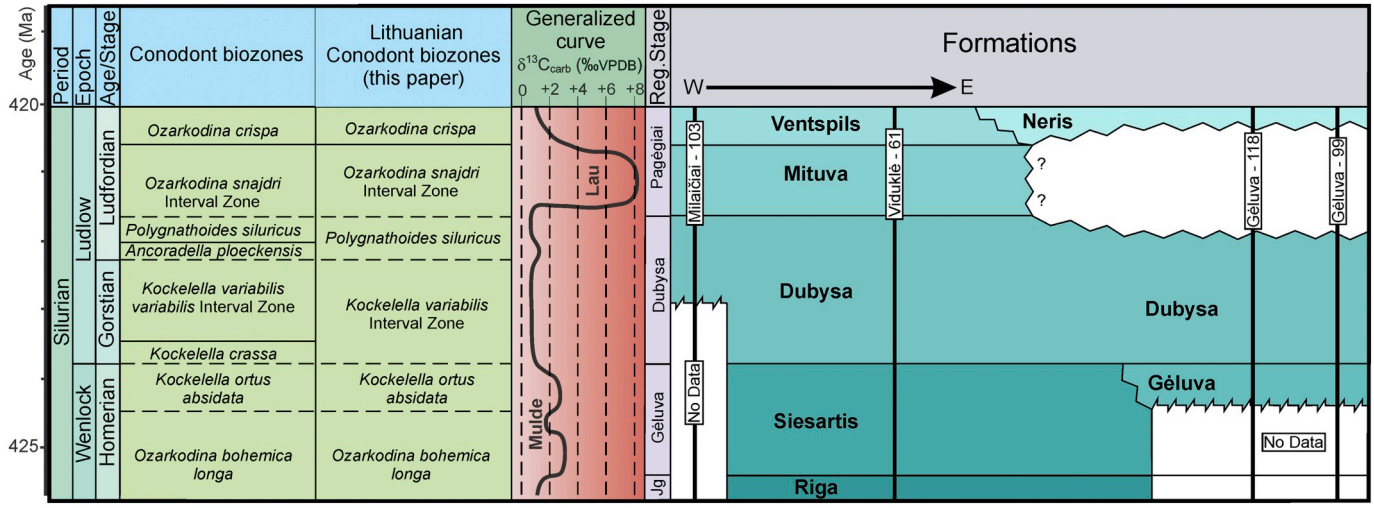

Fig. 10. Comparison of the stratigraphical patterns revealed in the study with the Silurian time scale and generalized $\delta^{13}C_{carb}$ curve (Cramer et al., 2011). Jg. – Jaagarahu Regional Stage.

Table 1
Average differences between synchronization lines and traditional Ludlow conodont biozone boundaries (in m).

Data preprocessing method	Comparison of the Viduklė-61 vs. focal cores	DTW	MWM
Raw data	Milaičiai-103	8.13	6.8
	Gėluva-99	22.03	23.73
	Gėluva-118	34.53	28.26
	Grand average	21.56	19.6
NMDS1 axis time series	Milaičiai-103	17.1	11.06
	Gėluva-99	15.16	19.36
	Gėluva-118	11.86	11.8
	Grand average	14.71	14.07

produced by using them. Evaluating the sufficiency of the sample sizes and later cooling part of the data is recommended. Interpolation (or other forms of data imputation) between the gaps left after reducing the data would be a necessary step in this analysis. Weighing the importance of the compared data points and corresponding entries in the primary distance matrices could be one more way forward in utilizing data of variable quality.

In this contribution, we described a stratigraphical correlation approach which utilized a pairwise comparison of conodont community turnover, not unlike a classical graphical biostratigraphical correlation, which performs comparisons of sections based on the distributions of first and last appearances of fossil species in 2 D (Shaw, 1964). Modern, graphical correlation-inspired techniques such as RASC and CONOP could provide solutions for first and last appearance event ordering problems by simultaneously analyzing hundreds of geological sections and stratigraphical composites (Sadler, 2004; Hammer and Harper, 2008; Crampton et al., 2018). Similarly, cross-recurrence plot-based correlation approaches could be extended to multiple dimensions by constructing N-dimensional cross-recurrence arrays. This step, in our opinion, should be a useful way forward in using quantitative and categorical paleoecological data for high resolution automated correlation of stratigraphic data, which is complimentary to traditional biostratigraphy and species first and last appearance event-based quantitative correlation.

6. Conclusions

The integrated stratigraphical and paleoecological comparative study of the Viduklė-61, Milaičiai-103, Gėluva-99 and Gėluva-118 deep section conodonts, and of the $\delta^{13}C_{carb}$, revealed that:

- The Gėluva-99 and Gėluva-118 sections of the Ludlow succession are characterized by a significant hiatus that spans the *Ozarkodina snajdri* Interval Zone and most probably the *Polygnathoides siluricus* Zone too.
- The time series of the non-metric multidimensional scaling scores for the conodont communities revealed that the Lau Event initiated a permanent state transition which can be easily detected in stratigraphically plotted time series, and used for correlating geological sections using cross-recurrence plots.
- Conodont compositional dynamics, as revealed by the recurrence and cross-recurrence plots, are characterized by sufficient spatial and temporal congruence in their turnover. This fact enables the use of compositional data in the high-resolution synchronization (geological correlation) of sections in the same region by applying dynamical time warping and newly developed moving window median recurrence point search algorithms.
- The greatest accuracy (as compared with the integrated stratigraphical model) in correlation with geological sections and utilizing conodont compositional diversity data in the cross-recurrence plots was achieved by using time series of NMDS1 scores that were obtained by analyzing a reduced dataset with sufficiently large sample sizes.

Acknowledgments

We would like to thank Editor Thomas Algeo for his detailed look at the manuscript and also managing Guest Editors in charge Annalisa Ferretti, Alyssa Bancroft and John Repetski for their invitation to contribute to this exciting “GECkO” special issue and for editorial suggestions. Two anonymous reviewers are sincerely thanked for their discussions on conodont stratigraphy, and for indicating a way forward from vague statements toward more operational approaches and more precise conclusions. This work is a contribution to the IGCP-652: “Reading geologic time in Palaeozoic sedimentary rocks: the need for an integrated stratigraphy.” The research of A.S. on the development of quantitative methods in paleoecology is supported by grant Research Council of Lithuania (09.3.3-LMT-K-712-02-0036). The research of R. S. on the recurrence patterns is supported by grant Research Council of Lithuania (09.3.3-LMT-K-712-03-0053). The research of L.A. and T. M. on the stable carbon isotopes was financed by the project IUT20-34 “The Phanerozoic journey of Baltica: sedimentary, geochemical and biotic signatures of changing environment – PalaeoBaltica.”

Appendix A. Supplementary data

Supplementary data to this article can be found online at https://doi.org/10.1016/j.palaeo.2019.03.029.

References

Abdi, Herve, 2007. Multiple correlation coefficient. In: Salkind, Neil (Ed.), Encyclopedia of Measurement and Statistics. Sage, Thousand Oaks (CA), pp. 648–651.

Aberhan, M., Kiessling, W., 2015. Persistent ecological shifts in marine molluscan assemblages across the end-Cretaceous mass extinction. Proc. Natl. Acad. Sci. 112, 7207–7212.

Agterberg, F.P., Gradstein, F.M., 1999. The RASC method for ranking and scaling of biostratigraphic events. Earth Sci. Rev. 46, 1–25.

Aldridge, R., Jeppsson, L., Dorning, K., 1993. Early Silurian oceanic episodes and events. J. Geol. Soc. 150, 501–513.

Allmon, W.D., 2001. Nutrients, temperature, disturbance, and evolution: a model for the late Cenozoic marine record of the western Atlantic. Palaeogeogr. Palaeoclimatol. Palaeoecol. 166, 9–26.

Allmon, W.D., Martin, R.E., 2014. Seafood through time revisited: the Phanerozoic increase in marine trophic resources and its macroevolutionary consequences. Paleobiology 40, 256–287.

Allmon, W.D., Yacobucci, M., 2016. Studying species in the fossil record: a review and recommendations for a more unified approach. In: Species and Speciation in the Fossil Record, pp. 59–120.

Alroy, J., 2000. New methods for quantifying macroevolutionary patterns and processes. Paleobiology 26, 707–733.

Bachan, A., Lau, K.V., Saltzman, M.R., Thomas, E., Kump, L.R., Payne, J.L., 2017. A model for the decrease in amplitude of carbon isotope excursions across the Phanerozoic. Am. J. Sci. 317, 641–676.

Bambach, R.K., 1993. Seafood through time: changes in biomass, energetics, and productivity in the marine ecosystem. Paleobiology 372–397.

Barrick, J.E., Kleffner, M.A., Karlsson, H.R., 2009. Conodont faunas and stable isotopes across the Mulde event (late Wenlock; Silurian) in southwestern Laurentia (south-central Oklahoma and subsurface west Texas). In: Over, D.J. (Ed.), Conodont Studies Commemorating the 150th Anniversary of the First Conodont Paper (Pander, 1856) and the 40th Anniversary of the Pander Society, pp. 41–56.

Barrick, J.E., Kleffner, M.A., Gibson, M.A., Peavey, F.N., Karlsson, H.R., 2010. The mid-Ludfordian Lau Event and carbon isotope excursion (Ludlow, Silurian) in southern Laurentia–preliminary results. Boll. Soc. Paleontol. Ital. 49, 13–33.

Bassett, M.G., Kaljo, D., Teller, L., 1989. The Baltic region. In: Holland, C., Bassett, M.G. (Eds.), A Global Standard for the Silurian System. National Museum of Wales Geological Series Cardiff, pp. 158–170.

Baud, A., Richoz, S., Pruss, S., 2007. The lower Triassic anachronistic carbonate facies in space and time. Glob. Planet. Chang. 55, 81–89.

Brazauskas, A., 1986. Silurian conodont communitites from Lithuania [in Russian]. In: Major Biotic Events in the History of Earth [in Russian], Talin, pp. 12–13.

Brazauskas, A., 1987. Silurian Conodont zones of Lithuania [in Russian]. Geologija 8, 40–58.

Brazauskas, A., 1993. Silurian Conodonts and Biostratigraphy of Lithuania [in Russian]. Vilnius University (Dissertation, 336 pp).

Calner, M., 2005. A Late Silurian extinction event and anachronistic period. Geology 33, 305–308.

Calner, M., 2008. Silurian global events–at the tipping point of climate change. In: Elewa, A. (Ed.), Mass Extinction. Springer, Berlin, pp. 21–57.

Calner, M., Eriksson, M.J., 2006. Evidence for rapid environmental changes in low latitudes during the late Silurian Lau Event: the Burgen-1 drillcore, Gotland, Sweden. Geol. Mag. 143, 15–24.

Calner, M., Jeppsson, L., 2003. Carbonate platform evolution and conodont stratigraphy during the middle Silurian Mulde Event, Gotland, Sweden. Geol. Mag. 140, 173–203.

Calner, M., Lehnert, O., Jeppsson, L., 2012. New chemostratigraphic data through the Mulde Event interval (Silurian, Wenlock), Gotland, Sweden. GFF 134, 65–67.

Chadimova, L., Vacek, F., Sobien, K., Slavik, L., Hladil, J., 2015. Petrophysical record of the Late Silurian shallow-water carbonate facies across the Lau Event (Prague Synform, Czech Republic) and dynamic time warping alignment of the magnetic susceptibility logs. Geol. Soc. Lond., Spec. Publ. 414, 133–155.

Chatalov, A., 2017. Anachronistic and unusual carbonate facies in uppermost Lower Triassic rocks of the western Balkanides, Bulgaria. Facies 63, 24.

Cisne, J.L., Rabe, B.D., 1978. Coenocorrelation: gradient analysis of fossil communities and its applications in stratigraphy. Lethaia 11, 341–364.

Cocks, L.R.M., Torsvik, T.H., 2005. Baltica from the late Precambrian to mid-Palaeozoic times: the gain and loss of a terrane's identity. Earth Sci. Rev. 72, 39–66.

Cooper, R.A., Sadler, P.M., Munnecke, A., Crampton, J.S., 2014. Graptoloid evolutionary rates track Ordovician–Silurian global climate change. Geol. Mag. 151, 349–364.

Corradini, C., Serpagli, E., 1999. A Silurian conodont zonation from late Llandovery to end Pridoli in Sardinia. Boll. Soc. Paleontol. Ital. 38, 255–273.

Corradini, C., Corriga, M.G., Männik, P., Schönlaub, H.P., 2015. Revised conodont stratigraphy of the Cellon section (Silurian, Carnic Alps). Lethaia 48 (1), 56–71.

Corriga, M.G., Corradini, C., Ferretti, A., 2009. Silurian conodonts from Sardinia: an overview. Rendiconti della Società Paleontologica Italiana 3, 95–107.

Corriga, M.G., Corradini, C., Walliser, O.H., 2014. Upper Silurian and lower Devonian conodonts from Tafilalt, southeastern Morocco. Bull. Geosci. 89 (1), 183–200.

Cramer, B.D., Kleffner, M.A., Saltzman, M.R., 2006. The late Wenlock Mulde positive carbon isotope (δ^{13}Ccarb) excursion in North America. GFF 128, 85–90.

Cramer, B.D., Brett, C.E., Melchin, M.J., Maennik, P., Kleffner, M.A., McLaughlin, P.I., Loydell, D.K., Munnecke, A., Jeppsson, L., Corradini, C., Brunton, F.R., Saltzman, M.R., 2011. Revised correlation of Silurian Provincial Series of North America with global and regional chronostratigraphic units and $\delta^{13}C_{carb}$ chemostratigraphy. Lethaia 44, 185–202.

Crampton, J.S., Cooper, R.A., Sadler, P.M., Foote, M., 2016. Greenhouse− icehouse transition in the late Ordovician marks a step change in extinction regime in the marine plankton. Proc. Natl. Acad. Sci. 113, 1498–1503.

Crampton, J.S., Meyers, S.R., Cooper, R.A., Sadler, P.M., Foote, M., Harte, D., 2018. Pacing of Paleozoic macroevolutionary rates by Milankovitch grand cycles. Proc. Natl. Acad. Sci. 115 (22), 5686–5691.

Dineen, A.A., Fraiser, M.L., Sheehan, P.M., 2014. Quantifying functional diversity in pre- and post-extinction paleocommunities: a test of ecological restructuring after the end-Permian mass extinction. Earth Sci. Rev. 136, 339–349.

Einasto, P.E., Abushik, A.F., Kaljo, D.L., Koren', T.N., Modzalevskaya, T.L., Nestor, H.E., Klaamann, E., 1986. Osobiennosti silurskogo osadkonakopleniya i associacii fauny v kraevych basseinach Pribaltiki i Podolii. In: Kaljo, D.L., Klaamann, E. (Eds.), Teoria i opyt ekostratigrafii. Valgus, Tallin, pp. 65–72.

Emsbo, P., 2017. Sedex brine expulsions to Paleozoic basins may have changed global marine 87Sr/86Sr values, triggered anoxia, and initiated mass extinctions. Ore Geol. Rev. 86, 474–486.

Eriksson, M.E., Nilsson, E.K., Jeppsson, L., 2009. Vertebrate extinctions and reorganizations during the late Silurian Lau Event. Geology 37, 739–742.

Foote, M., Miller, A.I., Raup, D.M., Stanley, S.M., 2007. Principles of Paleontology. Macmillan, New York (480 pp).

Frýda, J., Manda, Š., 2013. A long-lasting steady period of isotopically heavy carbon in the late Silurian ocean: evolution of the $\delta^{13}C$ record and its significance for an integrated $\delta^{13}C$, graptolite and conodont stratigraphy. Bull. Geosci. 88 (2), 463–482.

Gilinsky, N.L., 1994. Volatility and the Phanerozoic decline of background extinction intensity. Paleobiology 20, 445–458.

Girard, C., Renaud, S., 2007. Quantitative conodont-based approaches for correlation of the Late Devonian Kellwasser anoxic events. Palaeogeogr. Palaeoclimatol. Palaeoecol. 250, 114–125.

Gotelli, N.J., Graves, G.R., 1996. Null models in ecology. (Washington and London. 388 pp).

Hammer, Ø., Harper, D.A.T., 2008. Paleontological data analysis. John Wiley & Sons, Malden (368 pp).

Hammer, Ø., Harper, D.A.T., Ryan, P.D., 2001. PAST-PAlaeontological STatistics, ver. 3.18. Palaeontologia Electronica 4, 9.

Hinnov, L.A., Hilgen, F.J., 2012. Cyclostratigraphy and astrochronology. In: Gradstein, F.M., Ogg, J.G., Schmitz, M. (Eds.), The Geologic Time Scale 2012, 2-Volume Set. Elsevier, Amsterdam, pp. 63–83.

Hladil, J., Vondra, M., Cejchan, P., Robert, V., Koptikova, L., Slavik, L., 2010. The dynamic time-warping approach to comparison of magnetic-susceptibility logs and application to lower Devonian calciturbidites (Prague Synform, Bohemian Massif). Geol. Belg. 13 (4), 385–406.

Hladil, J., Slavik, L., Vondra, M., Koptikova, L., Cejchan, P., Schnabl, P., Adamovic, J., Vacek, F., Vich, R., Lisa, L., 2011. Pragian-Emsian successions in Uzbekistan and Bohemia: magnetic susceptibility logs and their dynamic time warping alignment. Stratigraphy 8 (4), 217–235.

Holland, S.M., 2017. Structure, not Bias. J. Paleontol. 91, 1315–1317.

Holland, S.M., Meyer, D.L., Miller, A.I., 2000. High-resolution correlation in apparently monotonous rocks: upper Ordovician Kope Formation, Cincinnati Arch. Palaios 15, 73–80.

Horn, H.S., 1966. Measurement of" overlap" in comparative ecological studies. Am. Nat. 100, 419–424.

Hull, P.M., Darroch, S.A.F., Erwin, D.H., 2015. Rarity in mass extinctions and the future of ecosystems. Nature 528, 345–351.

Jaeger, H., 1991. Neue Standard-Graptolithenzonenfolge nach der “Grossen Krise” an der Wenlock/Ludlow-Grenze (Silur). Neues Jahrb. Geol. Palaontol. Abh. 182, 303–354.

Jarochowska, E., Munnecke, A., 2016. Late Wenlock carbon isotope excursions and associated conodont fauna in the Podlasie Depression, eastern Poland: a not-so-big crisis? Geol. J. 51 (5), 683–703.

Jeppsson, L., 1990. An oceanic model for lithological and faunal changes tested on the Silurian record. J. Geol. Soc. 147, 663–674.

Jeppsson, L., 1997. The anatomy of the mid-early Silurian Ireviken Event and a scenario for PS events. In: Brett, C.E., a.B.G (Eds.), Paleontological Events: Stratigraphic, Ecological, and Evolutionary Implications. Columbia University Press, New York, pp. 451–492.

Jeppsson, L., 1998. Silurian oceanic events: summary of general characteristics. In: Landing, E.J.M. (Ed.), Silurian Cycles: Linkages of Dynamic Stratigraphy With Atmospheric, Oceanic and Tectonic Changes. New York State Museum, New York, pp. 239–257.

Jeppsson, L., 2005. Conodont-based revisions of the late Ludfordian on Gotland, Sweden. GFF 127, 273–282.

Jeppsson, L., Aldridge, R., 2000. Ludlow (late Silurian) oceanic episodes and events. J. Geol. Soc. 157, 1137–1148.

Jeppsson, L., Anehus, R., 1995. A buffered formic acid technique for conodont extraction. J. Paleontol. 69, 790–794.

Jeppsson, L., Calner, M., 2002. The Silurian Mulde Event and a scenario for secundo–-secundo events. Earth Environ. Sci. Trans. R. Soc. Edinb. 93, 135–154.

Jeppsson, L., Viira, V., Männik, P., 1994. Silurian conodont-based correlations between Gotland (Sweden) and Saaremaa (Estonia). Geol. Mag. 131, 201–218.

Jeppsson, L., Aldridge, R., Dorning, K., 1995. Wenlock (Silurian) oceanic episodes and events. J. Geol. Soc. 152, 487–498.

Jeppsson, L., Talent, J.A., Mawson, R., Simpson, A.J., Andrew, A.S., Calner, M., Whitford,

D.J., Trotter, J.A., Sandström, O., Caldon, H.-J., 2007. High-resolution Late Silurian correlations between Gotland, Sweden, and the Broken River region, NE Australia: lithologies, conodonts and isotopes. Palaeogeogr. Palaeoclimatol. Palaeoecol. 245, 115–137.
Jeppsson, L., Talent, J.A., Mawson, R., Andrew, A., Corradini, C., Simpson, A.J., Wigforss-Lange, J., Schönlaub, H.P., 2012. Late Ludfordian Correlations and the Lau Event, Earth and Life. Springer, pp. 653–675.
Kaljo, D., Boucot, A.J., Corfield, R.M., Le Herisse, A., Koren', T.N., Kriz, J., Männik, P., Märss, T., Nestor, V., Shaver, R.H., Siveter, D.J., Viira, V., 1996. Silurian bio-events. In: Walliser, O.H. (Ed.), Global Events and Event Stratigraphy in the Phanerozoic. Springer, Berlin, pp. 173–224.
Kidwell, S.M., 2001. Preservation of species abundance in marine death assemblages. Science 294, 1091–1094.
Kodama, K.P., Hinnov, L.A., 2014. Rock Magnetic Cyclostratigraphy. Wiley-Blackwell, Chichester (176 pp).
Koren', T.N., 1987. Graptolite dynamics in Silurian and Devonian time. Bull. Geol. Soc. Den. 35, 149–160.
Koren', T.N., Urbanek, A., 1994. Adaptive radiation of monograptids after the Late Wenlock crisis. Acta Palaeontol. Pol. 39, 137–167.
Kowalewski, M., Bambach, R.K., 2008. The limits of paleontological resolution. In: Harries, P.J. (Ed.), Approaches in High-Resolution Stratigraphic Paleontology. Kluwer Academic, New York, pp. 1–48.
Kozłowski, W., 2015. Eolian dust influx and massive whitings during the *kozlowski*/Lau Event: carbonate hypersaturation as a possible driver of the mid-Ludfordian Carbon Isotope Excursion. Bull. Geosci. 90, 807–840.
Kruskal, J.B., 1964. Nonmetric multidimensional scaling: a numerical method. Psychometrika 29, 115–129.
Lapinskas, P., 2000. Structure and Petroliferosity of the Silurian in Lithuania. Institute of Geology, Vilnius (203 pp).
Lazauskienė, J., Šliaupa, S., Brazauskas, A., Musteikis, P., 2003. Sequence stratigraphy of the Baltic Silurian succession: tectonic control on the foreland infill. Geol. Soc. Lond., Spec. Publ. 208, 95–115.
Lehnert, O., Eriksson, M.J., Calner, M., Joachimski, M., Buggisch, W., 2007a. Concurrent sedimentary and isotopic indications for global climatic cooling in the Late Silurian. Acta Palaeontol. Sin. 46, 249–255.
Lehnert, O., Frýda, J., Buggisch, W., Munnecke, A., Nützel, A., Kříž, J., Manda, S., 2007b. $\delta^{13}C$ records across the late Silurian Lau event: New data from middle palaeo-latitudes of northern peri-Gondwana (Prague Basin, Czech Republic). Palaeogeogr. Palaeoclimatol. Palaeoecol. 245, 227–244.
Lehnert, O., Männik, P., Joachimski, M.M., Calner, M., Frýda, J., 2010. Palaeoclimate perturbations before the Sheinwoodian glaciation: a trigger for extinctions during the 'Ireviken Event' Palaeogeogr. Palaeoclimatol. Palaeoecol. 296, 320–331.
Lenton, T.M., Dahl, T.W., Daines, S.J., Mills, B.J.W., Ozaki, K., Saltzman, M.R., Porada, P., 2016. Earliest land plants created modern levels of atmospheric oxygen. Proc. Natl. Acad. Sci. 113 (35), 9704–9709.
Lieberman, B.S., Melott, A.L., 2013. Declining volatility, a general property of disparate systems: from fossils, to stocks, to the stars. Palaeontology 56, 1297–1304.
Lieberman, B.S., MillerIII, W., Eldredge, N., 2007. Paleontological patterns, macro-ecological dynamics and the evolutionary process. Evol. Biol. 34, 28–48.
Loydell, D.K., 1998. Early Silurian sea-level changes. Geol. Mag. 135, 447–471.
Loydell, D.K., Jeppsson, L., Aldridge, R.J., 2001. Discussion on Ludlow (late Silurian) oceanic episodes and events Journal, Vol. 157, 2000, 1137–1148. J. Geol. Soc. 158, 731–732.
Makhnach, A.A., Kruchek, S.A., Pokrovsky, B.G., Strel'tsova, G.D., Murashko, O.V., Petrov, O., 2018. Carbon, oxygen, and sulfur isotope compositions and model of the Silurian rock formation in northwestern Belarus. Lithol. Miner. Resour. 53, 1–13.
Manda, Š., Frýda, J., 2014. Evolution of the late Ludlow to early Lochkovian brachiopod, trilobite and bivalve communities of the Prague Basin and their link with the global carbon cycle. GFF 136, 179–184.
Martma, T., Brazauskas, A., Kaljo, D., Kaminskas, D., Musteikis, P., 2005. The Wenlock-Ludlow carbon isotope trend in the Vidukle core, Lithuania, and its relations with oceanic events. Geological Quarterly 49, 223–234.
Marwan, N., Kurths, J., 2002. Nonlinear analysis of bivariate data with cross recurrence plots. Phys. Lett. A 302, 299–307.
Marwan, N., Thiel, M., Nowaczyk, N.R., 2002. Cross recurrence plot based synchronization of time series. Nonlinear Process. Geophys. 9, 325–331.
Marwan, N., Romano, M.C., Thiel, M., Kurths, J., 2007. Recurrence plots for the analysis of complex systems. Phys. Rep. 438, 237–329.
McKinney, M.L., Allmon, W.D., 1995. Metapopulations and disturbance: from patch dynamics to biodiversity dynamics. In: Erwin, D.H., Anstey, R.L. (Eds.), New Approaches to Speciation in the Fossil Record. Columbia University Press, New York, pp. 123–183.
Melchin, M.J., Koren', T.N., Štorch, P., 1998. In: Landing, E., Johnson, M. (Eds.), Global diversity and survivorship patterns of Silurian graptoloids. Silurian Cycles. New York State Museum Albany, pp. 165–182.
Melchin, M.J., Sadler, P.M., Cramer, B.D., 2012. The Silurian period. In: Gradstein, F.M., Ogg, J.G., Schmitz, M. (Eds.), The Geologic Time Scale 2012, 2-Volume Set. Elsevier, Amsterdam, pp. 525–558.
Meyers, S.R., Sageman, B.B., Pagani, M., 2008. Resolving Milankovitch: Consideration of signal and noise. Am. J. Sci. 308, 770–786.
Miller, C.G., Aldridge, R.J., 1997. *Ozarkodina remscheidensis* plexus conodonts from the upper Ludlow (Silurian) of the Welsh Borderland and Wales. J. Micropalaeontol. 16, 41–49.
Miller III, W., 2016. The species problem: concepts, conflicts, and patterns preserved in the fossil record. In: Allmon, W., Yacobucci, M. (Eds.), Species and Speciation in the Fossil Record. Chicago University press, Chicago, pp. 28–58.
Miller, A.I., Holland, S.M., Meyer, D.L., Dattilo, B.F., 2001. The use of faunal gradient analysis for intraregional correlation and assessment of changes in sea-floor topography in the type Cincinnatian. The Journal of Geology 109, 603–613.
Müller, M., 2007. Dynamic time warping. In: Information Retrieval for Music and Motion, pp. 69–84.
Munnecke, A., Delabroye, A., Servais, T., Vandenbroucke, T.R.A., Vecoli, M., 2012. Systematic occurrences of malformed (teratological) acritarchs in the run-up of Early Palaeozoic δ 13 C isotope excursions. Palaeogeogr. Palaeoclimatol. Palaeoecol. 367, 137–146.
Newman, M.E.J., Eble, G.J., 1999. Decline in extinction rates and scale invariance in the fossil record. Paleobiology 25, 434–439.
Olszewski, T.D., 2012. Remembrance of things past: modelling the relationship between species' abundances in living communities and death assemblages. Biol. Lett. 8, 131–134.
Paškevičius, J., 1997. The Geology of the Baltic Republics. Vilnius University and Geological Survey of Lithuania, Vilnius (387 pp).
Paškevičius, J., Lapinskas, P., Brazauskas, A., Musteikis, P., Jacyna, J., 1994. Stratigraphic revision of the regional stages of the Upper Silurian part in the Baltic Basin. Geologija (Vilnius) 17, 64–87.
Patzkowsky, M.E., Holland, S.M., 2012. Stratigraphic Paleobiology: Understanding the Distribution of Fossil Taxa in Time and Space. University of Chicago Press, Chicago (256 pp).
Porębska, E., Kozłowska-Dawidziuk, A., Masiak, M., 2004. The *lundgreni* event in the Silurian of the east European Platform, Poland. Palaeogeogr. Palaeoclimatol. Palaeoecol. 213, 271–294.
Puolamäki, K., Fortelius, M., Mannila, H., 2006. Seriation in paleontological data using Markov Chain Monte Carlo methods. PLoS Comput. Biol. 2, e6.
R Development Core Team, 2015. R: A Language and Environment for Statistical Computing. Version 3.1.3. R Foundation for Statistical Computing, Vienna.
Racki, G., Balinski, A., Wrona, R., Malkowski, K., Drygant, D., Szaniawski, H., 2012. Faunal dynamics across the Silurian-Devonian positive isotope excursions ($\delta^{13}C$, $\delta^{18}O$) in Podolia, Ukraine: Comparative analysis of the Ireviken and Klonk events. Acta Palaeontol. Pol. 57, 795–832.
Radzevičius, S., Spiridonov, A., Brazauskas, A., 2014Da. Integrated middle–upper Homerian (Silurian) stratigraphy of the Viduklė-61 well, Lithuania. GFF 136, 218–222.
Radzevičius, S., Spiridonov, A., Brazauskas, A., Norkus, A., Meidla, T., Ainsaar, L., 2014Db. Upper Wenlock $\delta^{13}C$ chemostratigraphy, conodont biostratigraphy and palaeoecological dynamics in the Ledai-179 drill core (Eastern Lithuania). Estonian Journal of Earth Sciences 63, 293–299.
Radzevičius, S., Spiridonov, A., Brazauskas, A., Dankina, D., Rimkus, A., Bičkauskas, G., Kaminskas, D., Meidla, T., Ainsaar, L., 2016. Integrated stratigraphy, conodont turnover and paleoenvironments of the Upper Wenlock and Ludlow of the Vilkaviškis-134 core (Lithuania). Newsl. Stratigr. 49 (2), 321–336.
Radzevičius, S., Tumakovaitė, B., Spiridonov, A., 2017. Upper Homerian (Silurian) high-resolution correlation using cyclostratigraphy: an example from Western Lithuania. Acta Geol. Pol. 67, 307–322.
Raup, D.M., Crick, R.E., 1979. Measurement of faunal similarity in paleontology. J. Paleontol. 1213–1227.
Ritterbush, K.A., Ibarra, Y., Bottjer, D.J., Corsetti, F.A., Rosas, S., West, A.J., Berelson, W.M., Yager, J.A., 2015a. Marine ecological state-shifts following the Triassic-Jurassic mass extinction. Paleontological Society Papers 21, 121–136.
Ritterbush, K.A., Rosas, S., Corsetti, F.A., Bottjer, D.J., West, A.J., 2015b. Andean sponges reveal long-term benthic ecosystem shifts following the end-Triassic mass extinction. Palaeogeogr. Palaeoclimatol. Palaeoecol. 420, 193–209.
Roopnarine, P.D., Angielczyk, K.D., 2015. Community stability and selective extinction during the Permian-Triassic mass extinction. Science 350, 90–93.
Ruban, D.A., 2017. Episodic events in long-term geological processes: a new classification and its applications. Geosci. Front. 9 (2), 377–389.
Sadler, P.M., 2004. Quantitative biostratigraphy-Achieving finer resolution in global correlation. Annu. Rev. Earth Planet. Sci. 32, 187–213.
Sadler, P.M., 2012. Integrating carbon isotope excursions into automated stratigraphic correlation: an example from the Silurian of Baltica. Bull. Geosci. 87, 681–694.
Sadler, P.M., Cooper, R.A., Melchin, M.J., 2009. High-resolution, early Paleozoic (Ordovician-Silurian) time scales. Geol. Soc. Am. Bull. 121, 887–906.
Saltzman, M.R., 2005. Phosphorus, nitrogen, and the redox evolution of the Paleozoic oceans. Geology 33, 573–576.
Saltzman, M.R., Thomas, E., 2012. Carbon isotope stratigraphy. In: The Geologic Time Scale. Elsevier, pp. 207–232.
Samtleben, C., Munnecke, A., Bickert, T., 2000. Development of facies and C/O-isotopes in transects through the Ludlow of Gotland: evidence for global and local influences on a shallow-marine environment. Facies 43, 1–38.
Scheffer, M., Carpenter, S.R., 2003. Catastrophic regime shifts in ecosystems: linking theory to observation. Trends Ecol. Evol. 18, 648–656.
Schmitz, B., Harper, D.A.T., Peucker-Ehrenbrink, B., Stouge, S., Alwmark, C., Cronholm, A., Bergström, S.M., Tassinari, M., Xiaofeng, W., 2008. Asteroid breakup linked to the Great Ordovician biodiversification event. Nat. Geosci. 1, 49–53.
Schönlaub, H.P., Corradini, C., Corriga, M.G., Ferretti, A., 2017. Chrono-, litho-and conodont bio-stratigraphy of the Rauchkofel Boden Section (Upper Ordovician–Lower Devonian), Carnic Alps, Austria. Newsl. Stratigr. 50 (4), 445–469.
Schubert, J.K., Bottjer, D.J., 1992. Early Triassic stromatolites as post-mass extinction disaster forms. Geology 20, 883–886.
Shaw, A.B., 1964. Time in Stratigraphy. McGraw-Hill Book Company, New York (365 pp).
Sheets, D.H., Mitchell, C.E., Izard, Z.T., Willis, J.M., Melchin, M.J., Holmden, C., 2012. Horizon annealing: a collection-based approach to automated sequencing of the fossil record. Lethaia 45, 532–547.

Sirota, J., Baiser, B., Gotelli, N.J., Ellison, A.M., 2013. Organic-matter loading determines regime shifts and alternative states in an aquatic ecosystem. Proc. Natl. Acad. Sci. 110, 7742–7747.
Slavik, L., Carls, P., 2012. Post-Lau Event (late Ludfordian, Silurian) recovery of conodont faunas of Bohemia. Bull. Geosci. 87, 815–832.
Slavik, L., Kříž, J., Carls, P., 2010. Reflection of the mid-Ludfordian Lau Event in conodont faunas of Bohemia. Bull. Geosci. 85, 395–414.
Spiridonov, A., 2017. Recurrence and Cross Recurrence Plots Reveal the Onset of the Mulde Event (Silurian) in the Abundance Data for Baltic Conodonts. The Journal of Geology 125, 381–398.
Spiridonov, A., Brazauskas, A., Radzevičius, S., 2015. The role of temporal abundance structure and habitat preferences in the survival of conodonts during the mid-early Silurian Ireviken mass extinction event. PLoS One 10, e0124146.
Spiridonov, A., Brazauskas, A., Radzevičius, S., 2016. Dynamics of abundance of the mid- to late Pridoli conodonts from the eastern part of the Silurian Baltic Basin: multifractals, state shifts, and oscillations. Am. J. Sci. 316, 363–400.
Spiridonov, A., Kaminskas, D., Brazauskas, A., Radzevičius, S., 2017a. Time hierarchical analysis of the conodont paleocommunities and environmental change before and during the onset of the lower Silurian Mulde bioevent – a preliminary report. Glob. Planet. Chang. 157, 153–164.
Spiridonov, A., Stankevič, R., Gečas, T., Šilinskas, T., Brazauskas, A., Meidla, T., Ainsaar, L., Musteikis, P., Radzevičius, S., 2017b. Integrated record of Ludlow (Upper Silurian) oceanic geobioevents–Coordination of changes in conodont, and brachiopod faunas, and stable isotopes. Gondwana Res. 51, 272–288.
Spiridonov, A., Venckutė-Aleksienė, A., Radzevičius, S., 2017c. Cyst size trends in the genus Leiosphaeridia across the Mulde (lower Silurian) biogeochemical event. Bull. Geosci. 92, 391–404.
Stigall, A.L., 2015. Speciation: expanding the role of biogeography and niche breadth in macroevolutionary theory. In: Macroevolution. Springer, pp. 301–327.
Stigall, A.L., Bauer, J.E., Lam, A.R., Wright, D.F., 2017. Biotic immigration events, speciation, and the accumulation of biodiversity in the fossil record. Glob. Planet. Chang. 148, 242–257.
Štorch, P., Manda, Š., Loydell, D.K., 2014. The early Ludfordian *leintwardinensis* graptolite event and the Gorstian–Ludfordian boundary in Bohemia (Silurian, Czech Republic). Palaeontology 57 (5), 1003–1043.
Stricanne, L., Munnecke, A., Pross, J., Servais, T., 2004. Acritarch distribution along an inshore–offshore transect in the Gorstian (lower Ludlow) of Gotland, Sweden. Rev. Palaeobot. Palynol. 130, 195–216.
Sullivan, N.B., McLaughlin, P.I., Emsbo, P., Barrick, J.E., Premo, W.R., 2016. Identification of the late Homerian Mulde Excursion at the base of the Salina Group (Michigan Basin, USA). Lethaia 49, 591–603.
Talent, J.A., Mawson, R., Andrew, A.S., Hamilton, P.J., Whitford, D.J., 1993. Middle Palaeozoic extinction events: faunal and isotopic data. Palaeogeogr. Palaeoclimatol. Palaeoecol. 104, 139–152.
Tetard, M., Monnet, C., Noble, P.J., Danelian, T., 2017. Biodiversity patterns of Silurian Radiolaria. Earth Sci. Rev. 173, 77–83.
Tomašových, A., Kidwell, S.M., 2010. Predicting the effects of increasing temporal scale on species composition, diversity, and rank-abundance distributions. Paleobiology 36, 672–695.
Tonarova, P., Eriksson, M.E., Hints, O., 2012. A jawed polychaete fauna from the late Ludlow Kozlowskii event interval in the Prague Basin (Czech Republic). Bull. Geosci. 87, 713–732.
Trotter, J.A., Williams, I.S., Barnes, C.R., Männik, P., Simpson, A., 2016. New conodont δ 18 O records of Silurian climate change: implications for environmental and biological events. Palaeogeogr. Palaeoclimatol. Palaeoecol. 443, 34–48.
Trubovitz, S., Stigall, A.L., 2016. Synchronous diversification of Laurentian and Baltic rhynchonelliform brachiopods: implications for regional versus global triggers of the Great Ordovician Biodiversification Event. Geology 44, 743–746.
Urbanek, A., 1993. Biotic crises in the history of Upper Silurian graptoloids: a palaeobiological model. Hist. Biol. 7, 29–50.
Urbanek, A., Radzevicius, S., Kozlowska, A., Teller, L., 2012. Phyletic evolution and iterative speciation in the persistent *Pristiograptus dubius* lineage. Acta Palaeontol. Pol. 57, 589–611.
Vandenbroucke, T.R.A., Emsbo, P., Munnecke, A., Nuns, N., Duponchel, L., Lepot, K., Quijada, M., Paris, F., Servais, T., Kiessling, W., 2015. Metal-induced malformations in early Palaeozoic plankton are harbingers of mass extinction. Nature Communications 6 (Article number: 7966).
Venckutė-Aleksienė, A., Radzevičius, S., Spiridonov, A., 2016. Dynamics of phytoplankton in relation to the upper Homerian (Lower Silurian) lundgreni event–an example from the Eastern Baltic Basin (Western Lithuania). Mar. Micropaleontol. 126, 31–41.
Vierek, A., Racki, G., 2011. Depositional versus ecological control on the conodont distribution in the Lower Frasnian fore-reef facies, Holy Cross Mountains, Poland. Palaeogeogr. Palaeoclimatol. Palaeoecol. 312, 1–23.
Viira, V., Einasto, R., 2003. Wenlock–Ludlow boundary beds and conodonts of Saaremaa Island, Estonia. In: Proceedings of the Estonian Academy of Sciences, Geology. Estonian Academy Publishers, pp. 213–238.
Vrba, E.S., 1993. Turnover-pulses, the Red Queen, and related topics. Am. J. Sci. 293, 418–452.
Vrba, E.S., DeGusta, D., 2004. Do species populations really start small? New perspectives from the Late Neogene fossil record of African mammals. Philosophical Transactions of the Royal Society B: Biological Sciences 359, 285–293.
Webber, C.L.J., Marwan, N., 2015. Recurrence Quantification Analysis: Theory and Best Practices.
Wood, R., Erwin, D.H., 2017. Innovation not recovery: dynamic redox promotes metazoan radiations. Biol. Rev. 93, 863–873.
Zenkner, L.J., Kozłowski, W., 2017. Anomalous massive water-column carbonate precipitation (whitings) as another factor linking Silurian oceanic events. GFF 139, 184–194.
Žigaitė, Ž., Joachimski, M.M., Lehnert, O., Brazauskas, A., 2010. $\delta^{18}O$ composition of conodont apatite indicates climatic cooling during the Middle Pridoli. Palaeogeogr. Palaeoclimatol. Palaeoecol. 294, 242–247.